MODELING FATIGUE BEHAVIOR OF 3D PRINTED TITANIUM ALLOYS

by

Sanket Kulkarni

A Thesis

Submitted to the Faculty of Purdue University

In Partial Fulfillment of the Requirements for the degree of

Master of Science in Mechanical Engineering

Department of Mechanical and Energy Engineering at IUPUI

Indianapolis, Indiana

August 2024

THE PURDUE UNIVERSITY GRADUATE SCHOOL
STATEMENT OF COMMITTEE APPROVAL

Dr. Jing Zhang, Chair
Department of Mechanical and Energy Engineering

Dr. Mangilal Agarwal
Department of Mechanical and Energy Engineering

Dr. Hamid Dalir
Department of Mechanical and Energy Engineering

Approved by:
Dr. Likun Zhu

Dedicated to my parents, family and to all the people who believed in me.

ACKNOWLEDGMENTS

I would like to thank Dr. Jing Zhang for constantly supporting and guiding me in this research work; I thank him for his patience and directing me in right direction during my Master's degree. I would also like to extend my gratitude towards Tejesh Dube and Sagar Sugrim who helped me understand research writing and the research process.

I will take this opportunity to thank Dr. Mangilal Agarwal for his support which helped me to complete this work. His motivation has helped me a lot to complete this work effectively.

I would also like to thank Dr. Hamid Dalir for being on my thesis committee and aiding me to complete this thesis.

TABLE OF CONTENTS

LIST OF TABLES

LIST OF FIGURES

LIST OF SYMBOLS

$\Delta\gamma_p^\alpha$ cyclic shear strain on slip plane.

k constant which controls peak normal stress

σ_n^α peak stress normal of slip plane.

σ_y macroscopic yield strength.

$\Delta\gamma_p^{max}$ maximum cyclic plastic shear strain

σ_n^{max} maximum normal stress

x initial instantiations

μ mean

σ standard deviation

ABSTRACT

Repeated loading and unloading cycles lead to the formation of strain in the material which causes initiation of the crack formation this phenomenon is called fatigue. Fatigue properties are critical for structures subject to cyclic load; hence fatigue analysis is used to predict the life of the material. Fatigue analysis plays an important role in optimizing the design of the 3D printed material and predicting the fatigue life of the 3D printed component.

The main objective of this thesis is to predict the fatigue behavior of different microstructures of Ti-64 titanium alloy by using the PRISMS-Fatigue open-source framework. To achieve this goal Ti-64 microstructure models were created using programming scripts, then the structures were exported to a finite element visualization software package, with all the required properties embedded in the pipeline. The PRISMS-Fatigue framework is used to conduct a fatigue analysis on 3D printed materials, using the Fatigue Indicator Parameters (FIP), which measure the driving force of fatigue crack formation in the microstructurally small crack growth.

Three different microstructures, i.e., cubic equiaxed, random equiaxed, and rolled equiaxed microstructures, are analyzed. The FIP results show that the cubic equiaxed grains have the best fatigue resistance due to their isotropic structural characteristics. Additionally, the grain size effect using 1 and 10 micrometers is investigated. The results show that the 1 micrometer grain size cubic equiaxed microstructure has a better fatigue resistance because as grains are small and they have a higher mechanical strength.

1. INTRODUCTION

1.1 Background

1.1.1 Fatigue

When material is subjected to a cyclic loading there is initiation and propagation of crack, this phenomenon crack propagation is known as fatigue. Once fatigue crack is initiated the crack propagates in small amount during each load cycle resulting into fracturing of the surface. First article on Fatigue life was published by Wilhelm Albert in 1837 [1].

Fatigue crack formation takes place in three stages namely: Crack initiation, Crack growth and Accelerated growth leading to ultimate failure of material. Crack initiation is the process where the material will develop the cell structure and harden because of constant applied load, this causes stress in that area to increase; and crack formation starts [2]. Crack grows because of constant loading of force which might be higher for the material which has developed the cell structure. Growth of crack is accelerated because of factors such as: higher mean stress effect, effect of surrounding environment on the material and short crack effect [1].

Fatigue Life is number of cycles under the specific load condition the material can sustain before the failure occurs [1]. Fatigue life can be predicted using different methods such as Miner's rule, Stress-life[2] method, Strain life method using these methods fatigue life prediction can be done.

Another method which can be used to analyze the crack formation in this thesis work the focus on crack formation method. Fatemi-Socie introduced one method to calculate the Fatigue behavior using FIPs [3].

1.1.2 Prisms Fatigue Framework

Prisms Fatigue Framework is an open-source software which is used to analyze the material behavior and use FIPs to generate the results [4]. Framework is based on crystal plasticity and is attached with various open-source software's to generate and visualize the microstructure [4].

Prisms Fatigue Framework comprises of five scripts 1). Generate microstructure, 2). Calculate FIPs, 3). Volume Averaged FIPs, 4). Compile and plot, 5). Multi axial gamma plane plot. These scripts execute and generate files which can be used by next script to generate results. Script generates .vtk files which can be used for visualization. It also generates. pickel files for data generation which is used by the framework to read and interpret the data.

1.1.3 Dream-3D

Dream-3D is the open-source software which helps the user to create the three-dimensional microstructure. It takes reference from the Crystal plasticity file which is used to create the model of microstructure and then convert it into a 3-D microstructure.

1.1.4 Para-view

Para-view is the software which is used to visualize the model which is been created it helps the users to visualize what effects are going in the microstructure. Para view also helps to visualize the flow of force in the microstructure which helps to spot FIPs in the microstructure or angle at which FIPs can be found.

1.1.5 Fatigue Indicator Parameters (FIPs)

Fatigue Indicator parameters are used to measure the driving force of fatigue crack formation in the microstructurally small crack growth [5]. Fatemi-Socie proposed the fatigue crack formation for critical plane based FIP of the form.

$$\mathrm{FIP}_{\alpha} = \frac{\Delta\gamma_{p}^{\alpha}}{2}\left[1 + k\frac{\sigma_{n}^{\alpha}}{\sigma_{y}}\right]$$

For this thesis work FIP’s formulated by Castelluccio and McDowell are used as they have proposed the effective version of crystallographic FIPs [5].

$$\mathrm{FIP}_{\mathrm{FS}} = \frac{\Delta\gamma_{p}^{\max}}{2}\left[1 + k\frac{\sigma_{n}^{\max}}{\sigma_{y}}\right]$$

1.2 Motivation

Fatigue analysis is a critical process used to evaluate the safety and durability of any structure or material that is subjected to cyclic loading. It involves analyzing the behavior of a component under repeated loading and unloading cycles to determine its resistance to fatigue failure.

In recent years, 3D printing technology has revolutionized the manufacturing industry by enabling the creation of intricate geometries that would be challenging or impossible to produce using traditional manufacturing methods. However, the layered nature of 3D-printed structures can introduce microstructural defects that significantly impact their mechanical properties, including their fatigue behavior.

As such, it is essential to conduct fatigue analysis on 3D-printed microstructures to assess their mechanical response to cyclic loading. This type of analysis can help to identify potential failure mechanisms, quantify fatigue damage accumulation, and predict the service life of 3D-printed components.

By understanding the fatigue behavior of 3D-printed microstructures, it is possible to optimize the printing process, design more reliable structures, and ensure the safety and durability of 3D-printed components in real-world applications. Therefore, fatigue analysis is an important tool for advancing the field of additive manufacturing and ensuring the safety and reliability of 3D-printed components in various industries.

1.3 Objective

This thesis intends to investigate and understand how TI-64 microstructure behave during fatigue. This work is crucial because 3D printing technology is becoming more and more popular for producing components with complex geometries and microstructures that are impractical for conventional manufacturing processes.

In this work, numerical simulations utilizing computational techniques like computer-aided engineering (CAE) software and finite element analysis (FEA) are used. The main objective of this thesis is to improve the fatigue resistance of 3D printed components with complex microstructures, such as refining printing parameters, implementing new materials, or creating unique microstructural characteristics.

The key objective of this research is to enhance the safety and dependability of complex microstructure 3D printed components, which are being used extensively in a variety of sectors, including consumer products, aerospace, automotive, and biomedicine. Engineers can design more safe and more dependable products, enhancing the overall performance and lifetime of these systems, by understanding the fatigue behavior of these components and creating better methods for estimating their fatigue life.

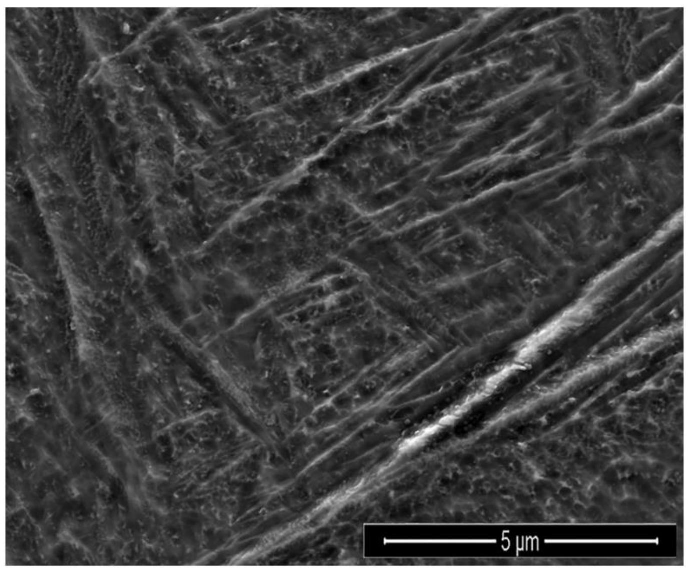

Figure 1.1. Experimental microstructure of Ti-64[6]

1.4 List of research task

1. Conducting a study on how different loading conditions affect the fatigue behavior of a particular material using Prism's Fatigue Framework.

2. Evaluating the accuracy and efficiency of Prism's Fatigue Framework in comparison with other fatigue analysis tools available in the market.

3. Developing innovative methods to improve the accuracy and reliability of fatigue analysis with Prism's Fatigue Framework, such as incorporating machine learning or optimizing input parameters.
4. Investigating how the microstructural characteristics of 3D printed components, such as grain size or orientation, impact their fatigue behavior using Prism's Fatigue Framework.

5. Exploring the capability of Prism's Fatigue Framework in predicting the residual life of components under various environmental conditions, such as temperature or humidity.

6. Analyzing how surface finishing techniques affect the fatigue behavior of metallic alloys using Prism's Fatigue Framework.

7. Developing new fatigue-resistant materials by optimizing the alloy composition and microstructure with Prism's Fatigue Framework.

8. Investigating how manufacturing defects, such as voids or cracks, influence the fatigue behavior of structural components using Prism's Fatigue Framework.

9. Studying the effect of load sequence and frequency on the fatigue behavior of composite materials using Prism's Fatigue Framework.

10. Examining the impact of mean stress on the fatigue behavior of materials with Prism's Fatigue Framework.

1.5 Structure of Thesis

An overview of the research topic, background, motivation, and research objectives would be given in the introduction section. The next step would be a review of the literature, which would include a more thorough discussion of the theoretical and practical facets of fatigue analysis .

The numerical modelling section would outline the approach to fatigue analysis, including the materials and test specimens used, the experimental or computational procedures, and the data analysis methods used. The methodology explains presumptions or restrictions and support the method of choice.

Results and analysis section present the findings of the fatigue analysis, including any experimental or computational data obtained. The results analyzed and interpreted in the context of the research objectives, highlighting any significant insights or key findings. The summary section summarizes the key findings and contributions of the study, their practical applications, and any limitations or recommendations for future research.

Additionally, appendices may be included, providing any supplementary information or data relevant to the study.

1.6 Literature Review

The field of fatigue analysis encompasses a wide range of research topics. Some of the key areas of research include the development of fatigue life prediction methods, the study of the mechanisms of fatigue failure, and the development of new materials and designs to mitigate the effects of fatigue.

One approach to fatigue life prediction is to use the concept of S-N curves, which plot the logarithm of the fatigue life in cycles against the applied stress range. The S-N curves have been developed for a range of materials and can be used to predict the life of a material subjected to a particular loading history.

Another approach to fatigue life prediction is using fracture mechanics, which models the initiation and growth of a crack under a cyclic loading condition. This method considers the properties of the crack and the material and can be used to predict the life of a component under complex loading conditions.

In addition to predicting the life of a material, the field of fatigue analysis also involves the study of the underlying mechanisms of fatigue failure. For example, researchers have studied the effects of stress concentrations, notches, and surface defects on fatigue life. They have also looked at the effects of corrosion and environmental factors on fatigue life.

Finally, the field of fatigue analysis also involves the development of new materials and designs to mitigate the effects of fatigue. For example, researchers have studied the use of composite materials, which exhibit lower vulnerability to crack initiation and growth, and the use of surface treatments to improve fatigue and wear resistance. They have also looked at the use of advanced manufacturing processes, such as additive manufacturing, to improve the structural integrity of components.

Researchers in this field have developed several methods for predicting the life of materials and components under cyclic loading conditions and have studied the mechanisms of fatigue and the development of new materials and designs to mitigate its effects.

The methods commonly used for fatigue analysis can be categorized as follows:

Damage Tolerance Method (DTM): This method considers the damage accumulation in the structure due to cyclic loading and assesses its structural integrity based on the damage state. It is suitable for the design of safe-life components where failure due to fatigue is non-catastrophic.[7] The damage tolerance method typically involves the following steps: Identification and characterization of microstructural features, such as grains, phases, precipitates, etc. Determination of the size, shape, and other properties of these features, such as orientation, volume fraction, aspect ratio, etc. Calculation of the stress distribution of these features in the local material coordinate system, using finite element analysis or other numerical methods. Calculation of the local stresses at specific critical locations within the microstructure, such as high-stress concentration areas or phase boundaries. Determination of the damage tolerance limits for these features, based on the size, shape, and material properties of the features and the stress distributions calculated in step 3 Comparison of the local stress levels to the damage tolerance limits to determine whether damage has occurred or is likely to occur during service. Calculation of the overall fatigue life of a component or structure, based on the size and distribution of the microstructural features, the damage tolerance limits, and the local stress levels. By considering both the size, shape, and material properties of individual features and the relationships between them, the damage tolerance method can provide a more detailed and accurate representation of fatigue behavior, which can lead to more accurate predictions of service life.[8]

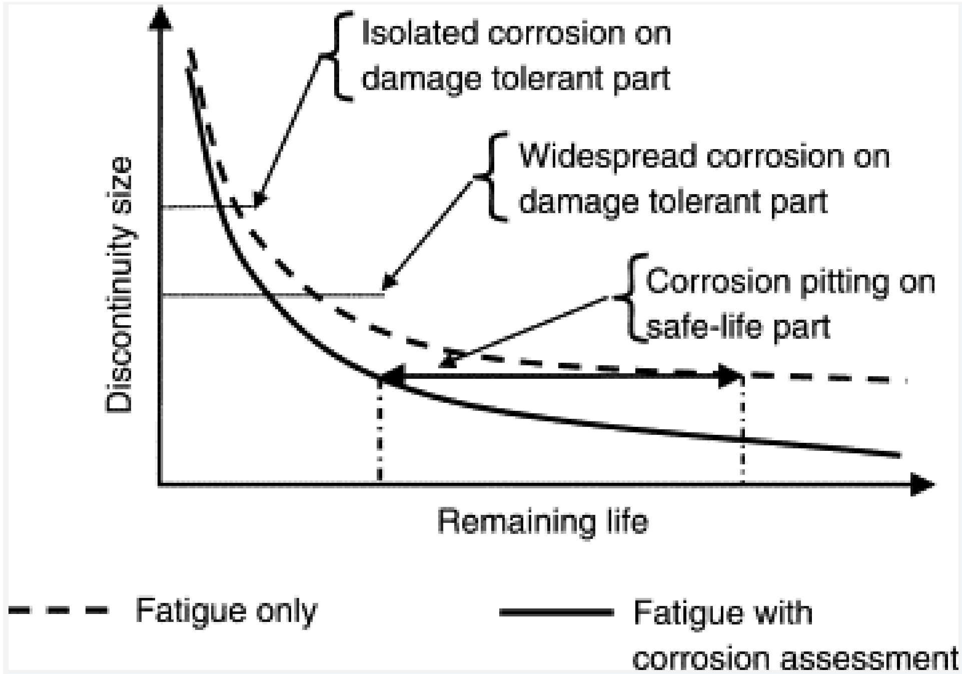

Figure 1.2. Damage Tolerance Method[8]

Finite Element Method (FEM): This method uses numerical techniques to calculate the stress-strain state of a structure subjected to cyclic loading. It is used for fatigue analysis of both components and structures. Through using FEM models, the structural system can be represented as a network of interconnected components. This technique accurately computes the levels of tension and distortion that ensue within these modules, hence being able to provide insights on how many cycles a given structure could endure before succumbing to fracturing.

The Finite Element Method (FEM) serves as a common tool used in fatigue analysis to mimic the performance of structures that endure cyclic loading. This modelling technique entails dissecting the structure into intricate components, wherein mechanics are then applied to each individual element. Such approach permits assessing stresses and strains within each element, eventually yielding comprehensive observations of the overall structural response.

There exist various ways of utilizing Finite Element Method (FEM) in the analysis of fatigue. One general method is implementing FEM to determine both stress and strain fields existing within a cyclically loaded structure. These fields may then be used for determining foreseeable life cycle of the structure, by deploying analytical techniques utilizing fatigue analysis such as the stress-life or strain-life approach.

Another avenue of examination is to utilize Finite Element Method (FEM) to replicate the progression of fissures in a configuration subjected to cyclic loading. The methodology includes representing the crack as a disjunction within the structure and applying FEM for computing the stress intensity factor in proximity to the crack apex. This stress intensity factor serves as an indicator for estimating both, rate of propagation of damage and remaining period before spontaneous rupture is likely to occur.

In terms of fatigue analysis, Finite Element Method (FEM) is an incredibly potent instrument. Its ability to simulate complex structures and predict the lifespan of such structures with a considerable degree of precision under cyclic loads has made it a highly valuable resource for engineers.

Experimental Method: This involves performing cyclic tests on a component or structure to observe its behavior under fatigue loading. It is used for validation of fatigue and structural analyze.[9]

The experimental method involves subjecting the material to a series of cyclic loading conditions, such as bending, torsion, or vibration. The number of cycles and the amplitude of the loading are carefully controlled to ensure that the material is subjected to a range of loading conditions that mimic real-world use. The fatigue life of the material is then determined based on the number of cycles required to cause failure.[9]

The experimental method is an important part of fatigue analysis because it allows engineers to test the material under real-world conditions and determine its fatigue life. It also provides valuable data that can be used to improve the design of the material and ensure that it can withstand the cyclic loading conditions that it will encounter in use.[9]

Threshold Stress (S-N) Curve: This method uses the relationship between nominal stress and the minimum number of cycles to failure (Nf) obtained from the experimental testing of the component or structure. The S-N curve is used to determine the design allowable stress and the fatigue life for the given material.[10]

Rainflow Cycle Counting: This method is used to calculate the average stress and strain in critical locations of a component or structure subjected to cyclic loading. It is used to determine the strain energy density and hence the fatigue life of a structural component.[11]

Life-Extension Method: This method is used to extend the fatigue life of a structural component by increasing the design allowable stress. It is commonly used for components that have already experienced a limited number of cycles of service.[12]

In addition to these methods, there are many other specialized techniques that can be used for specific applications, such as crack propagation analysis, residual stress analysis, and time-varying load analysis.

1.7 3D Printed Ti-64

3D Printed Ti-64 is manufactured by using two major additive manufacturing techniques: Selective Laser Melting (SLM); this technique uses high powered laser to fuse powdered metal layer by layer. [13] Electron Beam Melting (EBM); this technique uses an electron beam to melt and fuse the metal powder. [14] Manufacturing technique used in this work is Selective Laser Melting (SLM).

3D printed Ti-64 displays distinctive layered microstructure which influences mechanical properties and anisotropy of the microstructure. Additive manufacturing has rapid cooling rates which leads to formation of columnar grains growing perpendicular to the build direction. High cooling rates can produce martensitic α' phase, which is a metastable phase that can enhance hardness, but it can reduce ductility. Due to rapid solidification and thermal gradients, residual stresses can be developed within printed parts, which might affect dimensional accuracy and mechanical performance of the microstructure.

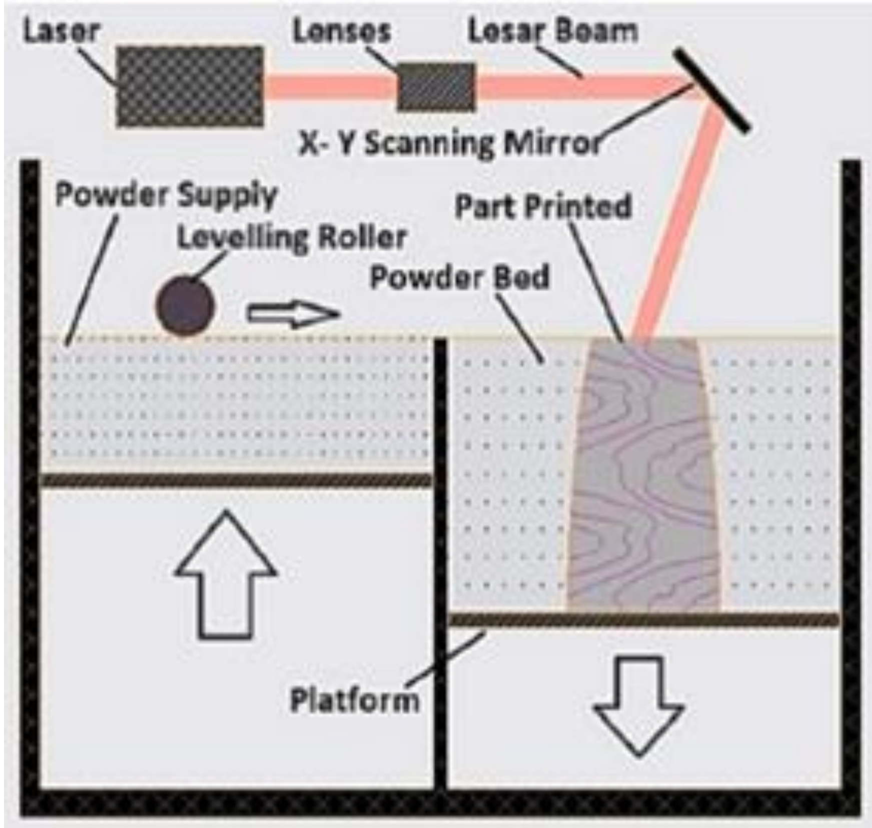

Figure 1.3. Selective Laser Melting (SLM)

Figure 1.3 represents the schematic process of how Selective Laser Melting work.
High powered laser (typically fiber lasers) is used, and power is adjusted to ensure that the powder receives sufficient energy to fully melt the Ti-64 powder particles. Laser operates in an inert gas environment (argon or nitrogen) to prevent oxidation of the titanium powder. Fine Ti-64 powder with a particle size that ranges between 1-10 micrometers is used. Powder bed is spread in thin layers (20-50 micrometers thick) over the platform. Levelling roller: rolls the new layer of Ti-64 over the previous layer this process repeats until the entire microstructure is built. For selective melting the laser scans the powder bed according to slice data, melting and fusing the Ti-64 powder particles to form a solid layer. The laser parameters like power, scan speed and hatch spacing is optimized to achieve full melting and minimize defects. Once build is complete, the part is encapsulated in loose powder, which is later removed by using vacuum system, brushes and compressed air. Post processing is done on material which include stress relieving, annealing and Hot Isostatic Pressing (HIP) to reduce residual stresses, to transform the microstructure and

eliminate porosity. Machining, grinding and polishing is done to improve surface roughness and fatigue performance.

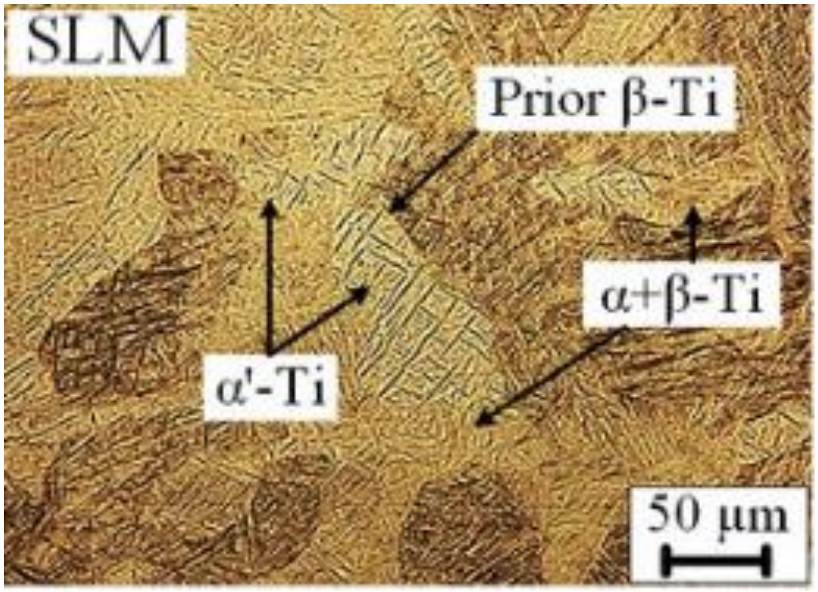

Figure 1.4. Ti-64 Microstructure Manufactured using SLM Method[[15]

Figure 1.4 depicts the 3D printed microstructure by considering the scale of microstructure as 50μm. This sizing helps to understand distribution of phases and microstructural features. α′ phase is martensitic phase that forms due to the rapid cooling rates during SLM process. This phase is needle-like or lath-like in structure and provides high strength but reduces ductility but can reduce the ductility of the microstructure.

Prior β-Ti this phase occurs in the microstructure because the microstructure experiences varying cooling rates leading to heterogeneous microstructure with regions of prior β-Ti and α + β-Ti phases. It also, initial BCC phase which occurs during high temperature phase of SLM.

α + β-Ti this region indicates the coexistence of both α and β phases, which are typical phases in Ti-6Al-4V after some amount of phase transformation from prior β-phase. The dual-phase region contributes to a balanced combination of strength and ductility in the alloy.

In SLM process material is built by layer-by-layer deposition and each layer can influence the microstructure of subsequent layers due to heat accumulation and thermal cycling. Post processing such as annealing or Hot Isostatic Pressing (HIP) can help transform the martensitic α' phase into more stable α + β microstructure, improving ductility and fatigue resistance.

Conventional Ti-64 is typically produced by forging, rolling and other thermomechanical processes. As discussed in this section 3D printed Ti-64 is manufactured using SLM method and EBM method.

Grain structure of conventional Ti-64 microstructure is controlled through heat treatments to achieve equiaxed grains or a lamellar structure. 3D printed Ti-64 often exhibits a layered structure with columnar grains growing perpendicular to the build direction due to rapid solidification.

Conventional Ti-64 mostly consists of a mixture of α (HCP) and β (BCC) phases. 3D printed Ti-64 can contain metastable α′ phase due to rapid cooling rates which can be converted to the α+β structure through post-processing.

Conventional Ti-64 is generally more uniform and homogeneous microstructure due to controlled processing. 3D printed Ti-64 is more heterogeneous in comparison with conventional Ti-64 microstructure will experience potential defects like porosity and residual stresses.

Strength of 3D printed Ti-64 is slightly higher than conventional Ti-64 due to presence of the martensitic α′ phase both the microstructure has similar ultimate tensile strength which is around 1100 MPa.

Ductility of 3D printed Ti-64 is lower than conventional Ti-64 due to residual stresses and microstructural inhomogeneities; elongation at break can be 8-14% in comparison with conventional microstructure which has elongation at around 10-15%. Hardness of conventional Ti-64 is lower than 3D printed Ti-64, but it can be tailored through heat treatment.

2. NUMERICAL MODELLING

2.1 Overview

Prisms Fatigue framework uses Prisms Crystal Plasticity finite element method (CPFEM) to create model along with the strain in uniaxial tension- compression and simple shear and pure shear [5]. Dream-3D instantiations are used to generate realistic microstructures using data from CPFEM model [2]. Defining custom fatigue indicator parameters in prisms fatigue and last step would be implementing the slip systems in post-processing of FIP calculations [5].

2.2 Crystal Plasticity Finite Element Method (CPEM)

CPEM which is used for carrying out experimental results in this process is used as defined in the work done by Tang Gu, Krzysztof S. Stopka and David L. McDowell [5]. Ti-6Al-4V(Ti64) consist of Critical Resolved Shear Stress (CRSS) which account for active slip planes in the microstructure. Parameters taken into consideration for calibrating the microstructure.

Table 2.1. Updated Flow Control Parameter [5]

Flow Rule Parameter	**Strain Calibration**
$CRSS_{Basal}$	339 MPa
$CRSS_{Prismatic}$	266 MPa
$CRSS_{Pyramidal<a>}$	450 MPa
$CRSS_{Pyramidal<a+c>}$	551 MPa
Softening term	42 MPa
Asymetry-Sensitivity η	22

2.3 Microstructure Parameters

Dream.3D is uses the CPEM model which is been created to generate Statistical Volume Elements (SVEs) [16]. SVEs are cubic with elemental size of $(30)^3$ and volume of $(300mm)^3$ [5]. The average log normal grain size is 60mm with standard deviation of 15mm [16]. Microstructure is setup in such a way that there are 264 SVE per grain. Composition of the microstructure is set to be 50% a phase and 50 % a+b colony [17]. Uniaxial straining cycle are applied at 300K temperature at straining amplitude of 0.8% and straining rate of 10^{-3} s^{-1} which promotes elastic-plastic shakedown. The strain amplitude corresponds to HCF conditions, below the polycrystal yield point [5].

2.4 Banding Scheme

Banding is like meshing the microstructure, banding divides the grain size in varied sizes and shapes. Most accurate banding is sub-banding as its emphasis constant volume averaging scheme. FIPa is calculated at every integration point of the SVE for each slip plane system [17].

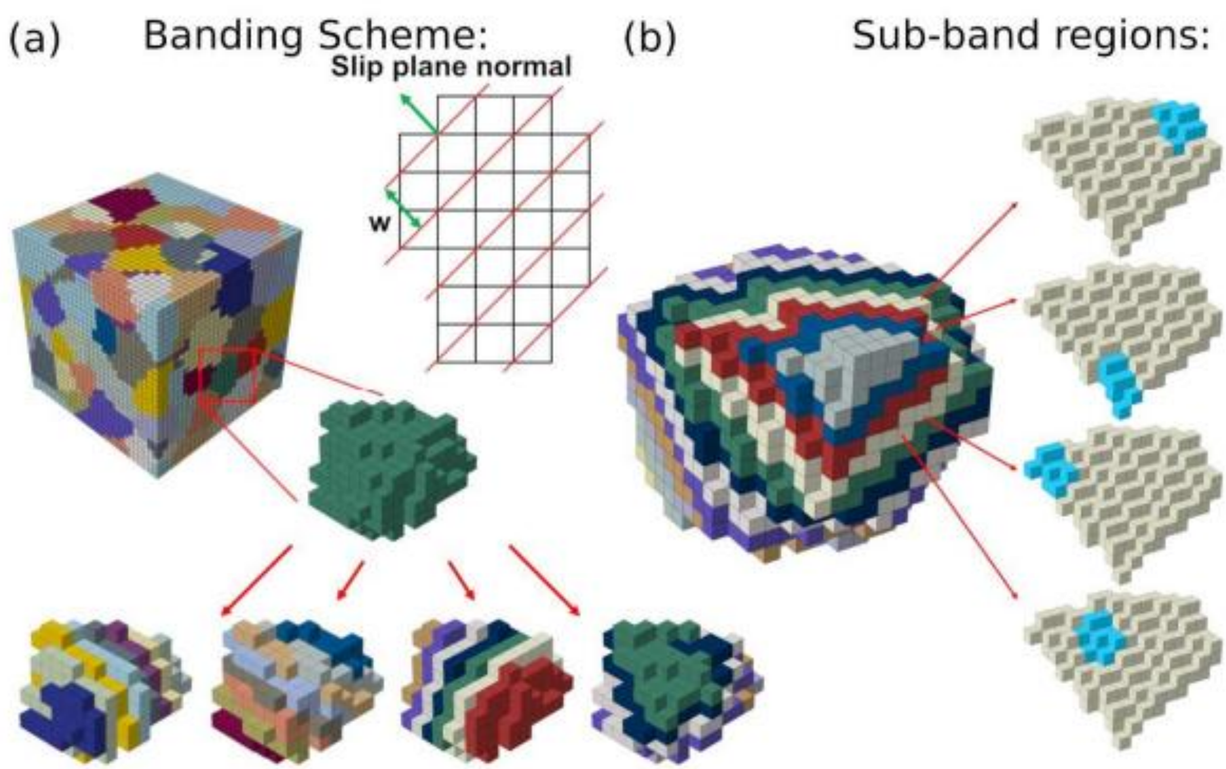

Figure 2.4. Banding Explanation [17]

2.5 Gumbel EVD for plotting results.

For plotting of results Extreme Value Distribution FIPs has been used, which help to generate the plots with varying probability region. Code is designed in such a way that extreme value is determined which is been chosen over a threshold limit, randomly chosen variables follow Gumbel EVD to generate the plot results [16].

$$-\ln\left[-\ln\left(F_X(\mu, \sigma, x)\right)\right] = \frac{x - \mu}{\sigma}$$

3. RESULTS AND DISCUSSIONS

3.1 3-D Microstructure Generated

Visualization of a 3-D microstructure which is created using generate microstructure prisms script. In this visualization we can spot and visualize boundaries and grain created using Dream-3d and prisms plasticity model as well as generate microstructure prisms fatigue script. As shown in 3.1.

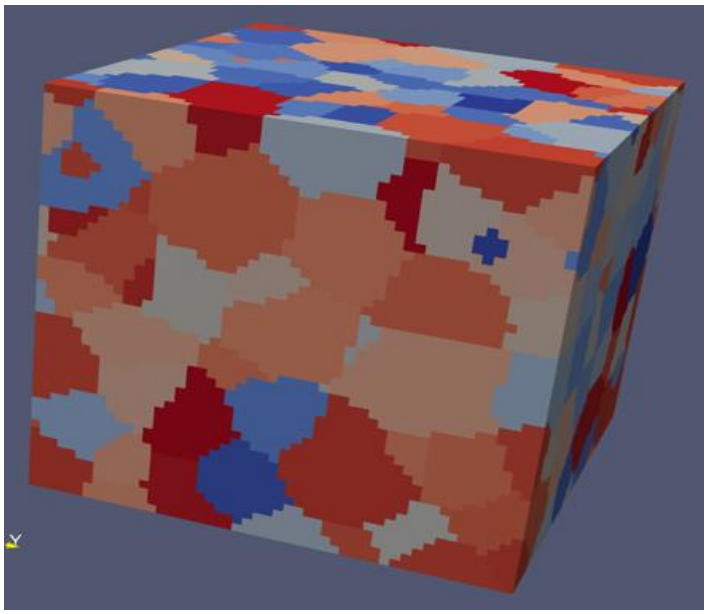

Figure 3.1. Microstructure Generated

3.2 Cubic Equiaxed Microstructure

In cubic equiaxed microstructures, grains or crystal regions exhibit approximate equiaxed shapes with cubic symmetry and have approximately the same shape. The grains are essentially cubic in shape and do not have preferential alignment or elongation in this microstructure. An equiaxed cubic structure consists of cubic grains that are similar in size and shape, forming a three-dimensional network. Processing techniques can be used to create this microstructural arrangement, or it can occur naturally. This microstructure contains cubic grains, which have an equiaxed shape that is roughly cubic in length, width, and height. These grains are not elongated or flattened and display no preferential orientation. Cubic equiaxed grains are randomly oriented with respect to each other with no preferred alignments or crystallographic orientations. Since there is no preferred orientation of grains, cubic equiaxed microstructure generally results in isotropic material properties. In a cubic equiaxed microstructure, grain boundaries are irregular in shape and have varying crystallographic orientations. Material properties like mechanical strength, diffusion rates, and crack propagation resistance depend greatly on these grain boundaries. Cubic equiaxed microstructures promote homogeneity throughout the material, as there are no predominant orientations/densities. This can result in more consistent material behavior and properties. Fig 3.2. figure shows 250 grains which are cubic equiaxed and are generated using the dream-3d file and can be visualized using Para view.

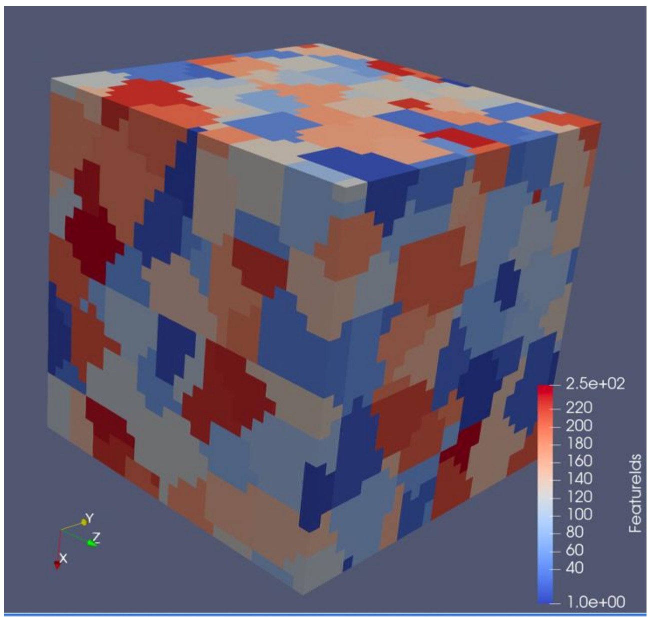

Figure 3.2. Cubic Equiaxed

3.3 Random Equiaxed

In a random equiaxed microstructure, grains or crystals are randomly distributed and have about equiaxed shapes within the material. There is no preferential alignment or elongation in equiaxed grains. Materials with random distributions of equiaxed grains may have isotropic mechanical properties, which is contrary to materials with anisotropic microstructures that vary across directions. Typically, grain boundaries in equiaxed microstructures are irregular and may have varying orientations. Particle boundary sliding, diffusion, and crack propagation are influenced by grain boundary characteristics, including structure, mobility, and energy. Equiaxed grains promote homogeneity in the material, as there are no specific orientations or regions of high density or low density. This can lead to more consistent material behavior and properties. 2-d microstructure is created in dream-3d and then they are visualized in Para View using, using generate microstructure prisms fatigue script which generates .vtk file. As shown in Fig 3.3.

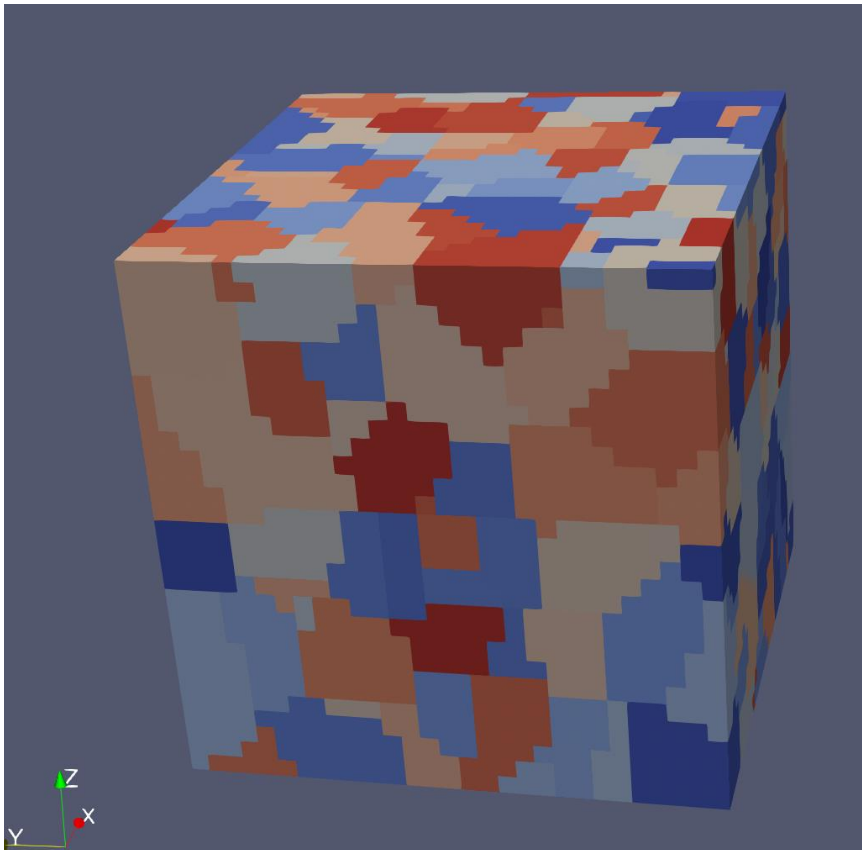

Figure 3.3. Random Equiaxed

3.4 Rolled Equiaxed Microstructure

During rolling, Ti-6Al-4V often exhibits elongated grains known as "prior β grains" or "primary α phases." The elongation occurs because of deformation caused by rolling. A flattened appearance is produced by these elongated grains align along the rolling direction. Recrystallized β grains or secondary α phases are typically found within elongated grains. When rolling occurs, plastic deformation occurs, causing recrystallization to occur. When recrystallization occurs, new equiaxed grains are formed with a random orientation and become more refined than the original grains. As well as elongated grains, equiaxed grains play a significant role in mechanical properties of rolled Ti-6Al-4V alloys. Elongated grains provide strength and anisotropic mechanical behavior along the rolling direction, while equiaxed grains enhance toughness and ductility. This type of microstructure is shown in Fig 3.4.

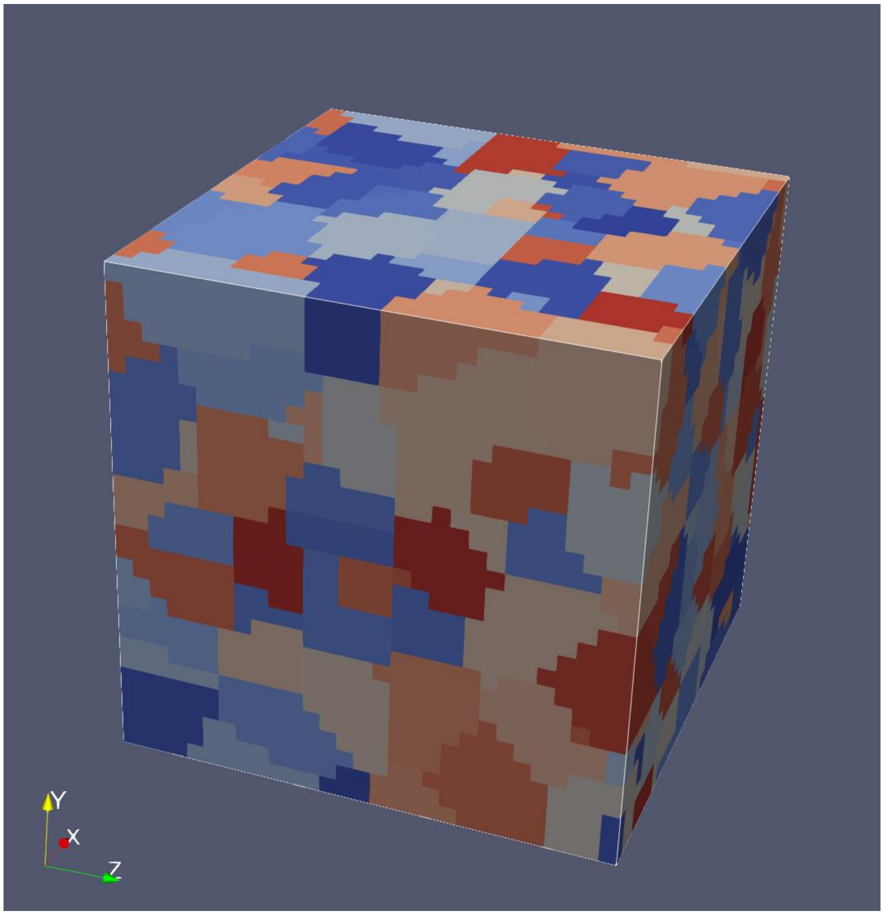

Figure 3.4. Rolled Equiaxed

It is evident in Figure 3.4. grain structure appears to be elongated. It also shows α phase is predominantly present throughout the microstructure, which helps to predict that microstructure has weak fatigue resistance.

Figure 3.5 shows the experimental image of Rolled Equiaxed Ti-64 alloy at the scale size of 20μm.

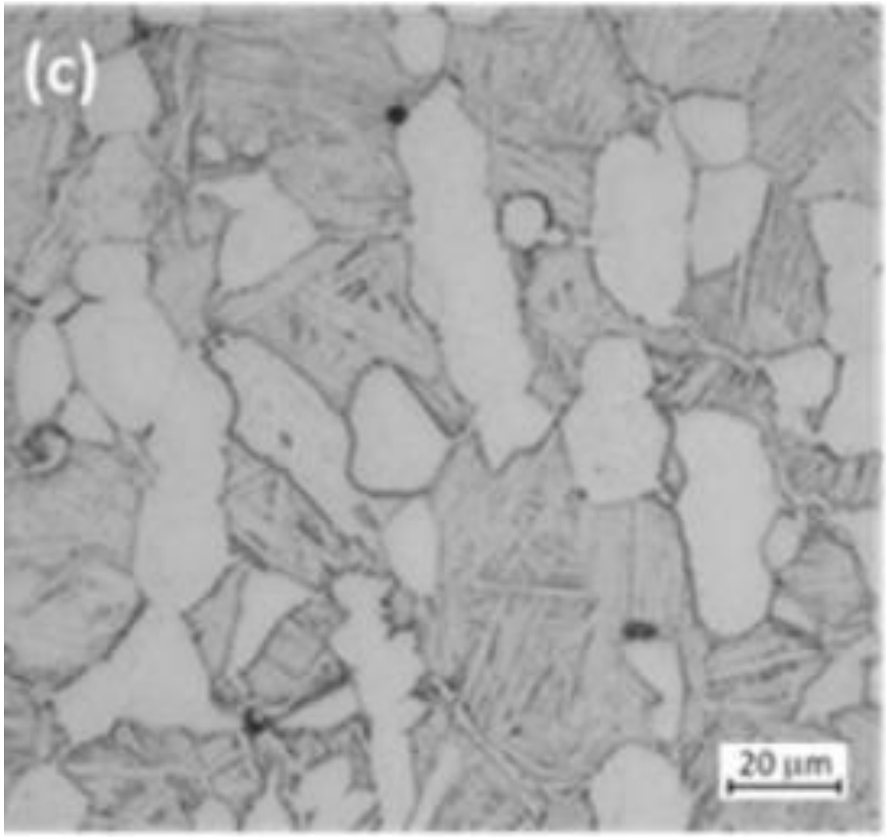

Figure 3.5. Experimental Rolled Equiaxed Microstructure[18]

There is presence of elongated or equiaxed α phase which can be clearly seen as lighter regions. The darker region in the microstructure represents β phase of the microstructure which has body-centered cubic (BCC) structure. Lath- like or needle-like structure represent characteristics of the martensitic α' phase formed during rapid cooling.

In Ti-64 α phase contributes to the alloy's strength and creep resistance. Martensitic α' phase contribute to hardness and strength but may reduce ductility of the alloy. The retained β enhances ductility of the microstructure.

As it can be observed from the grain structure in Figure 3.5 the lighter region i.e. α phase has elongated grains and dominates the texture of microstructure. Second most dominating texture is needle-like or lathe-like structure, which suggests that the microstructure has significant presence of α'. There is less presence of β region. This microstructural experiment resembles to the model shown in Figure 3.4.

It can be predicted that microstructure will be hard and will have strength, but residual stresses in the microstructure will be higher which will lead to less fatigue resistance and microstructure would will have poor performance under cyclic loading.

3.5 Banding Visualization

The banding in the material refers to alternating regions of different properties or appearances because of differences in its microstructure. By employing appropriate sample preparation techniques, such as metallographic polishing, and choosing suitable etchants, the microstructure can be observed. Banding can be visualized better with DIC microscopy or polarized light microscopy, which enhance the contrast between different regions of the microstructure. In this visualization the microstructure is volume averaged and sub-banded on the 24 slip planes of Ti-64 material. Bands are seen in blue color which then can be used for calculating the FIPs in the microstructure. As shown in Fig 3.6.

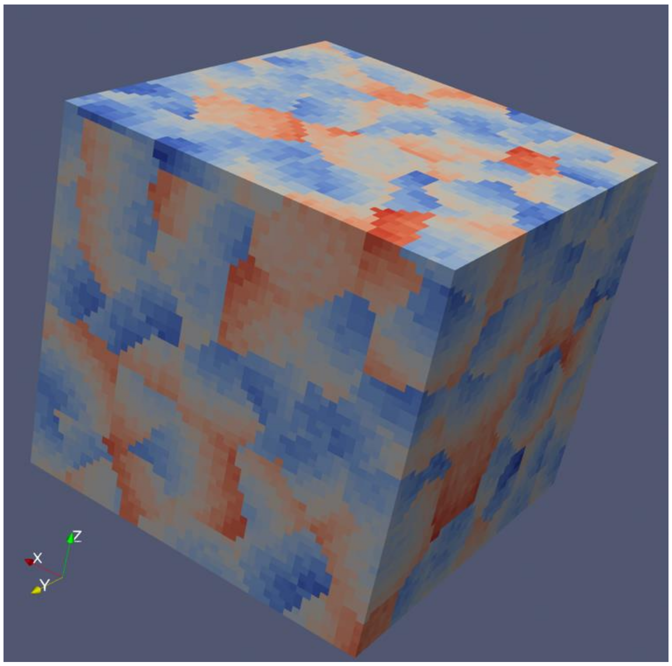

Figure 3.6. Banding

3.6 Strain Flow in Microstructure

In a strain flow plot, two-dimensional axes represent microstructural features of a material, such as grain orientation, grain boundaries, and other relevant structure features. Microstructures are characterized using microscopy, electron backscatter diffraction, and digital image correlation (DIC) to create the strain flow plot before and after cyclic loading. Different microstructural regions may experience local strains or deformations.[19] It can be seen as areas or regions within a microstructure where strains tend to localize or concentrate. A localized strain region can trigger fatigue crack initiation and propagation. In these regions of microstructure, strains or deformations tend to increase, suggesting that they are more prone to fatigue crack initiation. A better understanding of fatigue initiation sites is essential for predicting fatigue life. Strain flow plot can highlight the dominant deformation mechanisms operating within the material during cyclic loading. It can show the pathways and modes of plastic deformation, such as slip, twinning, or grain boundary sliding, which influence the fatigue behavior of the material. Fig 3.6 shows the visualization of strain flow in the microstructure. Visualization gives Euler angles which helps to analyze the microstructure and predict at which locations the Maximum FIPs would be formed.

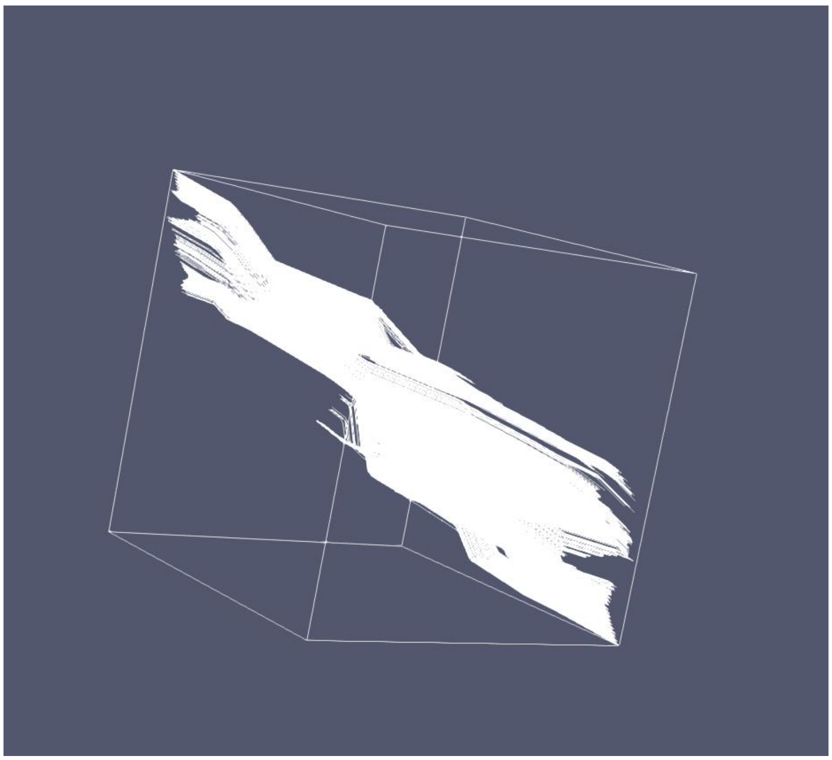

Figure 3.7. Strain stream flow

Figure 3.6 is a 3D plot within a cubic boundary, showing the distribution and direction of strain flow within the microstructure. Strain flow is concentrated along a specific plane, which indicate there might be a slip plane or region of localized deformation.

Orientation of the strain flow is diagonal across the cube which indicates that the material is experiencing combination of shear and normal stresses, leading to an oblique strain flow pattern.

White regions in the plot indicate that the areas of high concentrations and which imply that material is undergoing plastic deformation and indicating the initiation and propagation of a shear band or a crack. Based on the plot it can be predicted that the material is higher stress in the central region as it appears to be more elongated indicating that crack initiation will start from the center of the material.

As the strain flow progresses there it can be predicted that the material is seeing the dislocation motion from α phase into β phase as the lower half of the plot is accommodating higher strain and providing strength by enhancing fatigue resistance of the alloy.

3.7 Visualization FIPs calculated in 3-D microstructure.

FIPs are calculated based on the volume averaged bands and 3-D visualization helps to find the maximum elemental FIPs in the microstructure. As shown in Fig.3.8. Maximum Elemental FIPs occur at 0.0086.

Figure 3.8. depicts the color map indicating the Fatigue indicator parameters for the material under cyclic loading. Color map on the right-hand side ranges from blue to red, representing different magnitudes of FIPs. Max value is 8.6×10^{-3} and is associated with dark red color, Min value is 1.1×10^{-4} and is associated with dark blue color.

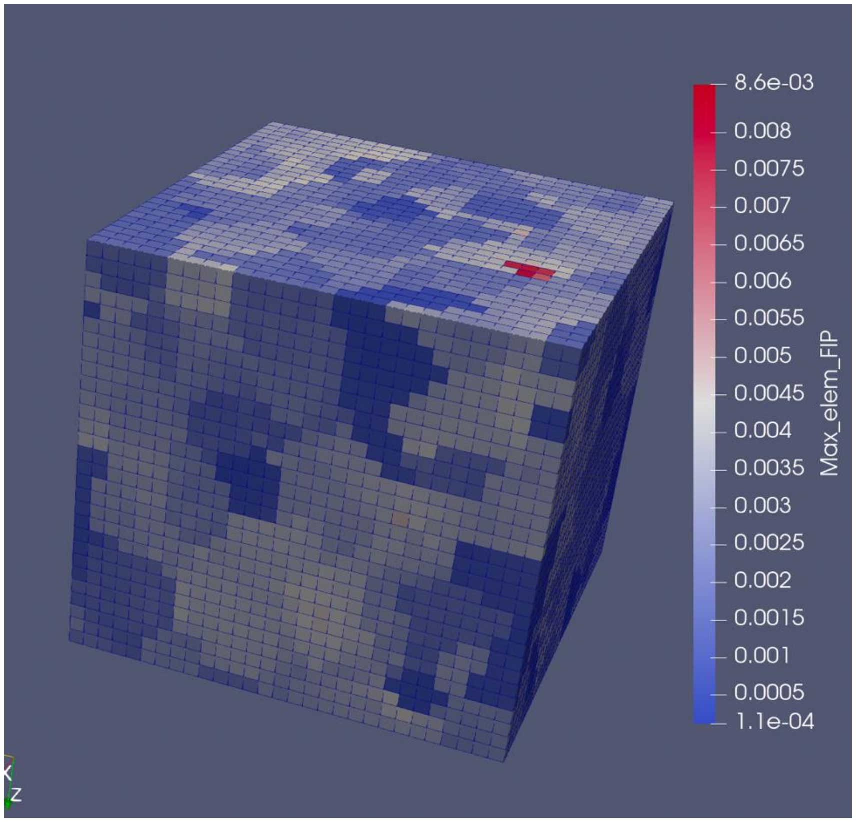

Figure 3.8. Visualization FIPs calculated in 3-D microstructure.

Cubic microstructure is divided into small voxels and depending on the strain experienced by the material the Fatigue Indicator Parameters are developed in the material; dark blue areas represent the less development of FIPs and dark red represents higher development of FIPs.

High strain areas are concentrated in the red regions which are likely to be critical sites for damage initiation, such as crack formation or fatigue failure. Blue regions indicate the areas with low strain and less likely to experience immediate failure.

Heterogeneous distribution of parameter suggests the presence of α and β phases influencing how strain is distributed. Based on the plot it can be predicted that regions with high strain would be concentrated in and around α phase as it is more brittle and more prone to failure under cyclic loading. Areas with low strain will be reach in the β phase as strain distributes more evenly because β phase is more ductile and can accommodate more strain. Light red region in the plot depicts at there is existence of both α and β phases and it can be predicted that damage has slowed down in that region.

3.8 Graphical Representation of FIPs in sub-banded microstructure

Prisms Fatigue Framework works on a schematic representation of the sub-banded microstructure, using the main features as focus. The sub-banded microstructure consists of alternating bands of different phases. Bands related to Ti-6Al-4V can be labeled as α and β for the specific phases they represent. Localized phase transformations induced by cyclic loading are usually the cause of these FIPs, which can be easily identified by identifying certain locations within the sub-bands with distinct symbols. Color-coding sub-bands and FIP locations can help distinguish α and β phases and microstructural regions. The phases could be represented by different shades of gray or distinct colors. In contrast, a contrasting color can be used to highlight FIP locations. The orientation or direction of the FIPs within the microstructure can be represented by arrows or lines. This can allow to examine how FIPs propagate. FIPs w.r.t -ln(-ln(p)) plot shows the probability of FIPs plotted in the microstructure for each instantiation and for Cubic Periodic, Cubic Free Surface, Random Periodic, Random Free Surface, Rolled Periodic and Rolled Free Surface type and result has been plotted.

X-axis of the plot shown in Figure 3.9. represents Fatigue Indicator Parameter (FIP), which is used to predict fatigue damage. The values are in the order of 10^{-2}. Y-axis represents transformed version of probability density function of FIP values, often used in extreme value statistics to assess the distribution of extreme values. Plotting this comparison will help to predict the highest FIP values which are critical for fatigue analysis.

Filled red circles represent cubic microstructure with periodic boundary conditions, open red circles represent cubic microstructure with free surface microstructure boundary conditions. Filled blue squares represent random periodic microstructure, open blue squares represent random free surface microstructure. Filled green triangles represent rolled periodic microstructure, open green triangles represent rolled free surface boundary condition.

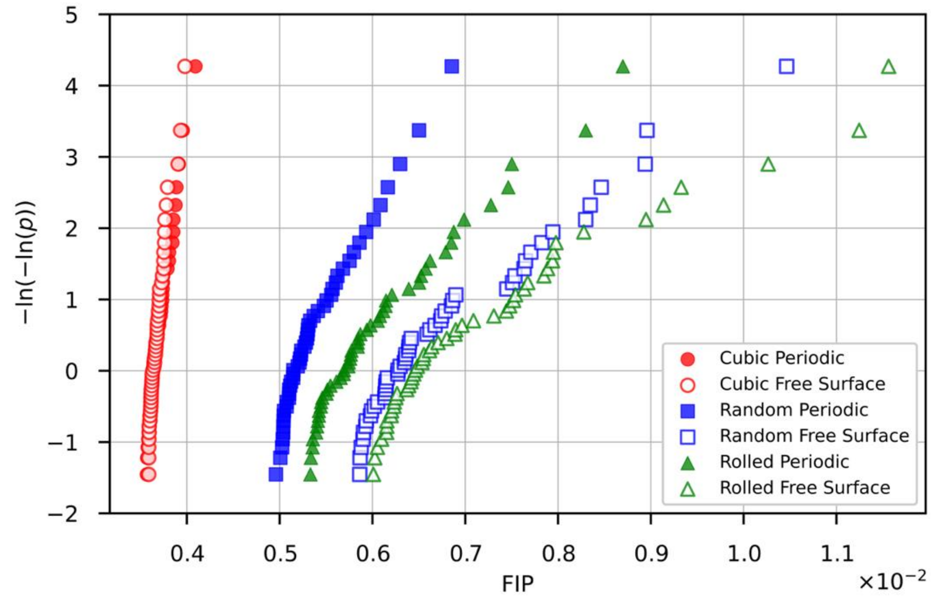

Figure 3.9. Graphical Representation of FIPs in sub-banded region.

Data points are clustered into groups based on the microstructure and boundary conditions. Each group depicts a distinct range of FIP values and probability density transformations.

Based on the plot it can be predicted that both cubic and free surface boundary conditions for cubic microstructures show lower FIP values, with the cubic free surface data (open circles) having more concentrated distribution compared to the periodic one (filled circles).

Random microstructures both periodic and free surface, show higher FIP values than the cubic microstructures. The free surface condition (open squares) tends to have more scattered and higher FIP values compared to the periodic condition (filled squares).

Rolled microstructure exhibit highest FIP values as compared to both cubic and random microstructures. Periodic condition (filled triangles) shows relatively high FIP values but are less scattered as compared to free surface condition.

Based on the plot it can be predicted that Ti-64 microstructures which have periodic boundary conditions are more clustered and possibly have lower FIP values indicating less extreme strain localization. Free surface boundary conditions tend to produce more scattered and higher FIP values, which suggests that microstructure has higher strain localization and potential sites for fatigue crack initiation.

3.9 Graphical Representation of Shape Factors in sub-banded microstructure

Shape Factors are geometrical characteristics measured in the sub-bands. These include aspect ratio, circularity, elongation, or area fraction. The shape factors can be calculated for each microstructural feature based on the defined parameters. Using appropriate equations or algorithms, the Shape Factors can be calculated for all relevant regions. Sub-bands or regions should be mapped with different colors according to their shape factor values. Using a gradient color scheme, darker and more intense colors represent higher shape factor values. Display's color legend or scale to explain each color's shape factor value. This legend helps viewers understand the range of values. A plot or chart combining microstructure visualization and shape factor values can be generated. The microstructure can be visualized by overlaying it on the chart. For example, each sub-band could be represented by a Shape Factor value in a scatter plot. Appropriate axes labels and titles are used to clarify the Shape Factor parameters, units, and any other relevant information. Ensure the plot is clearly labeled and easy to interpret. Include any necessary annotations or additional information on the plot to provide context or highlight specific details. FIPs w.r.t -ln(-ln(p)) plot shows the probability of FIPs of different shape function is plotted in the microstructure for each instantiation and for Cubic Periodic, Cubic Free Surface, Random Periodic, Random Free Surface, Rolled Periodic and Rolled Free Surface types and result has been plotted.

X-axis of the plot shown in Figure 3.10. represents Fatigue Indicator Parameter (FIP), which is used to predict fatigue damage. The values are in the range of $4x10^{-3}$ to $8x10^{-3}$. Y-axis represents transformed version of probability density function of FIP values, often used in extreme value statistics to assess the distribution of extreme values. Plotting this comparison will help to predict the highest FIP values which are critical for fatigue analysis.

Filled red circles represent cubic microstructure with equiaxed grains, open red circles represent cubic microstructure with elongated grains. Filled blue squares represent random microstructure, with equiaxed grains open blue squares represent random microstructure with elongated grains.

Filled green triangles represent rolled microstructure with equiaxed grains, open green triangles represent rolled microstructure with elongated grains.

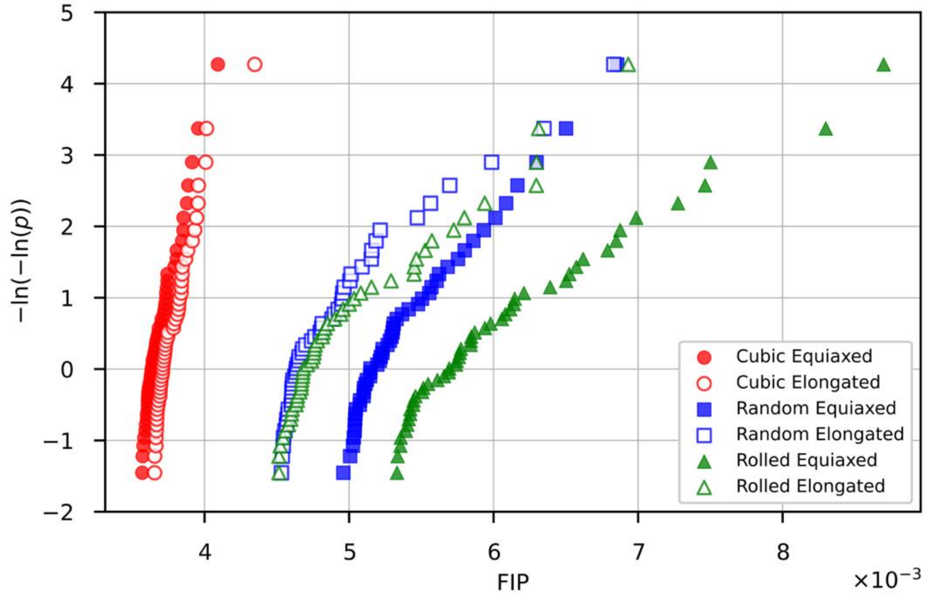

Figure 3.10. Graphical Representation in Shape Factor.

Data points are clustered into groups based on the type of microstructure (cubic, random, rolled) and grain shape (equiaxed vs. elongated). Each group depicts a distinct range of FIP values and probability density transformations.

Cubic microstructures with equiaxed grain shape (Filled Circles) have lowest FIP values, indicate that it has better resistance of fatigue damage. Cubic microstructure with elongated grain shape (Open Circles) are more prone to fatigue damage showing higher FIP values in the plot.

Random microstructures with equiaxed grain shape (Filled Squares) have higher FIP values than cubic equiaxed and elongated microstructure indicating that random equiaxed microstructure has moderate fatigue resistance. Random microstructures with elongated grain shape (Open Squares) have higher FIP values than equiaxed counterparts showing they are more susceptible to fatigue damage.

Based on the plot Rolled microstructure with equiaxed grain shape (Filled Triangles) have higher FIP values compared to both random and cubic equiaxed microstructures. Rolled microstructures with elongated grain shape (Open Triangles) have highest FIP values among all the other shapes.

Based on the plot it can be predicted Ti-64 with Equiaxed grain shape will show better fatigue resistance due to uniform strain distribution within the grain. Elongated grains show higher FIP values suggesting that the microstructure is experience anisotropic strain and potential stress concentration in elongated direction make it more prone to fatigue damage. It can also be elongated grain might show dominance of α phase within the microstructure.

3.10 Distance of FIPs from Free surface

A measurement of the distance between each FIP location in the sub-bands and the free surface can be accomplished by calculating the shortest path along the microstructure. Within sub-banded microstructures, to create a graph or graphical representation that illustrates how far FIPs are from free surfaces. A data point represents an FIP location within a microstructure. It is possible to plot the FIP values and the distance from the free surface. You should customize the plot by adding appropriate labels, axes titles, and a legend. This will ensure clarity and make the plot easy to follow. The plotted data will reveal trends, correlations, or patterns that relate the FIP values to their distance from the free surface. As a result of the microstructure's proximity to the free surface, FIPs may occur or behave differently depending on its location. FIPs w.r.t Distance from the free surface is plotted Fig 3.10 shows the distance at which FIPs are formed from the free surface of the microstructure. This helps to predict the distance at which FIPs can be spotted.

The plot in Figure 3.11. shows the change in FIP values as a function of distance from the free surface, which are more critical for predicting fatigue life of microstructure by taking into consideration effect of surface and subsurface interaction under cyclic loading. X-axis represents (Distance from the free surface [2, 13]) and Y-axis represent FIPs which help to predict the fatigue damage of the microstructure throughout the depth. Values range from 0.4×10^{-2} to 1.2×10^{-2}.

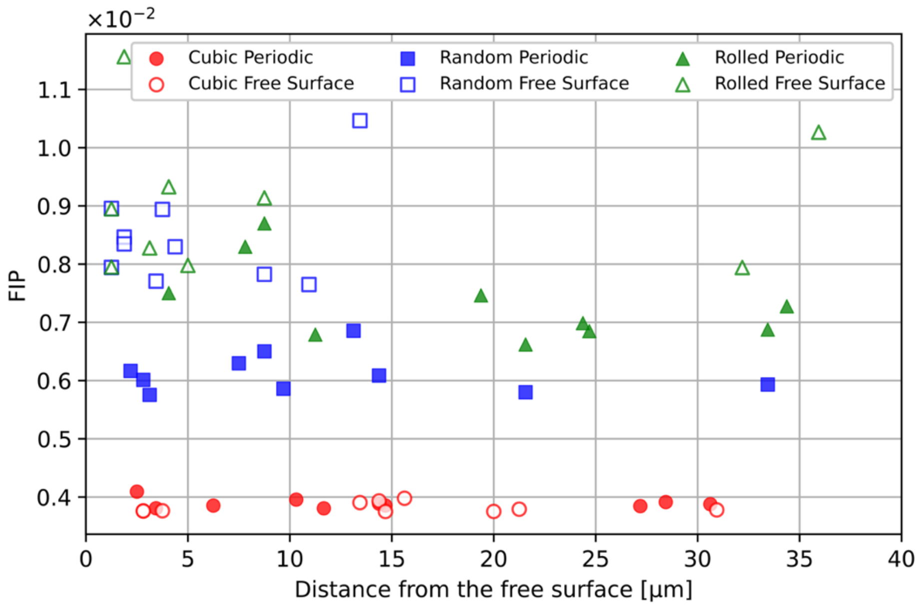

Figure 3.11. Distance of FIPs from Free surface.

Filled red circles represent cubic microstructure with periodic boundary conditions, open red circles represent cubic microstructure with free surface microstructure boundary conditions. Filled blue squares represent random periodic microstructure, open blue squares represent random free surface microstructure. Filled green triangles represent rolled periodic microstructure, open green triangles represent rolled free surface boundary condition.

Cubic microstructure with periodic boundary conditions (Filled Circles) shows consistently low values (around $0.4\text{x}10^{-2}$) indicating good fatigue resistance throughout the depth of microstructure. Cubic microstructure with free surface boundary conditions (open circles) shows similar values, suggesting that fatigue damage do not significantly increase for cubic microstructures.

Random microstructure with periodic boundary conditions (Filled Squares) has higher FIP values ranging from 0.5 to 0.7×10^{-2} indicating that it is more susceptible to fatigue damage compared to cubic microstructures. Random microstructures with free surface (Open squares) have higher FIP values up to $1.1\text{x}10^{-2}$ indicating that microstructure has increased fatigue damage near the free surface.

Rolled microstructure with periodic boundary conditions (Filled Triangles) have high values ranging from 0.6 to 0.9 $\times 10^{-2}$ indicating significantly higher susceptibility for fatigue damage. Rolled microstructure with free boundary conditions (Open Triangles) have the greatest susceptibility to fatigue damage.

Based on the plot it can be predicted that Ti-64 with periodic boundary conditions result in lower FIP values and indicating less fatigue damage. It can also be predicted that fatigue damage is more near the surface, suggesting that the free surface increases stress concentration and fatigue susceptibility.

3.11 Gamma Plane Simulation

Gamma Plane Simulations are carried out for multiaxial shear strain and are plotted to predict the fatigue life of microstructure. Uniaxial stresses are plotted on middle line, biaxial stresses are plotted on the upper line and triaxial is plotted on the lower line. Gamma plane plot closely resembles with Brown and Miller's theory which can be used to predict fatigue life [20].

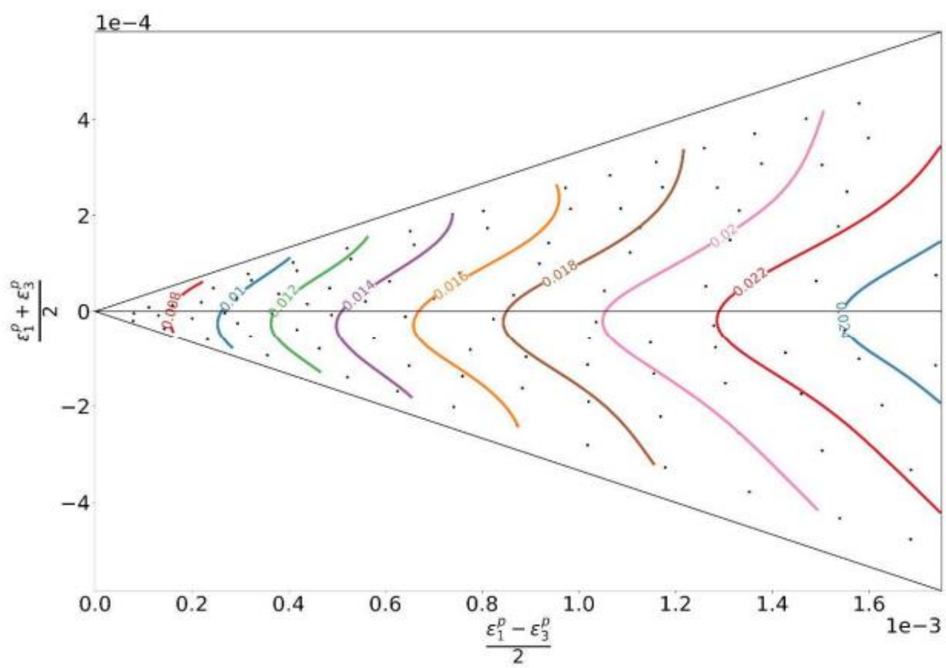

Figure 3.13. Gamma Plane Simulation.

Figure 3.13. represents the gamma plane plot for Ti-64. In this plot X-axis represents differential plastic strain between two principal directions and Y-axis represent average plastic strain between two principal directions. Contour Lines represent levels of specific strain parameter, potentially indicating strain energy or equivalent plastic strain. Triangular region defines bonds within which the strain components interact.

The triangular region is outlined by solid lines represents the permissible range of the strain components within the microstructure. The boundaries of this triangles are dictated by the physical constraints or symmetries in material's deformation and behavior.

Contour lines represent levels of a certain strain parameter (potentially strain energy density or equivalent plastic strain, as they move from the center outwards, suggesting higher deformation or strain energy accumulation. The plot exhibits symmetry along the horizontal axis indicating that the material responds similarly to positive and negative differences in the plastic strain components.

Colors and values help to visualize how strain is distributed within the material, regions with denser contour line indicate areas with higher gradient in the strain parameter, pointing to regions of significant strain localization or deformation.

3.12 Fatigue Analysis for Different Grain Sizes

In this section there is comparison of different grain size of a 3D printed Ti-64. The grain sizes for carrying out the comparison are considered for As-printed condition and the manufacturing technique used is Selective Laser Method (SLM). Typical grain sizes range between 1 micrometer to 10 micrometer. Post processing methods are not considered while comparing the microstructure as it can be application specific. [21] Fine grains are columnar in nature, aligned with the build direction. Higher laser power and slower scan speeds generally lead to larger melt pools and slower cooling rates, which results in coarser grains.

3.12.1 Average Grain Size of 10μm

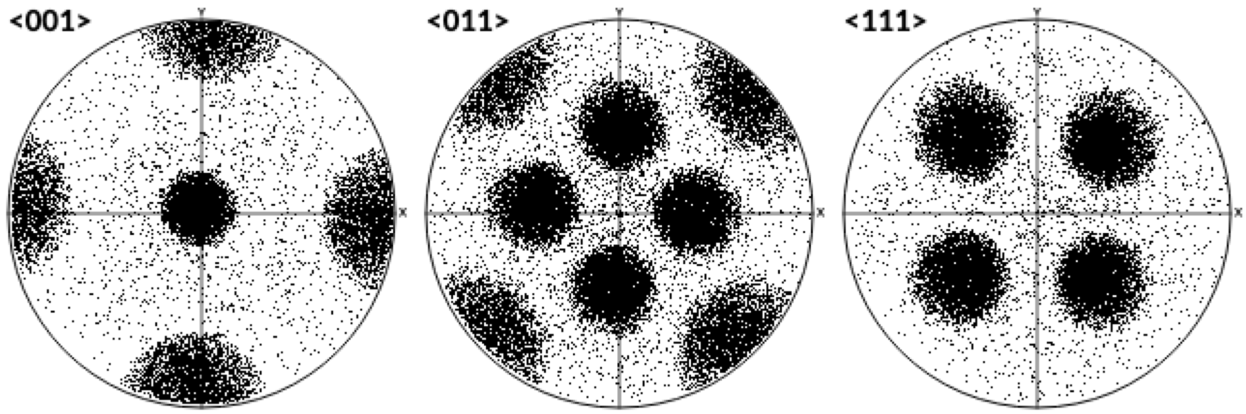

Figure 3.14. Polar Figure of Ti-64 with 10μm Grain Size

Figure 3.14 shows Polar Figure of Ti-64 with 10μm grain size. This figure represents the projections which are used to represent the crystallographic orientation distribution of grains in polycrystalline materials. Three circles represent a different crystallographic direction which are: ⟨001⟩, ⟨011⟩, and ⟨111⟩.

⟨001⟩ Pole Figure (Left Circle) this pole figure shows four high-intensity spots at the poles of the circle and one high intensity spot at the center. This indicates that many grains are oriented such that their axis aligns with these directions. The symmetry suggests a cubic crystal structure as ⟨001⟩ is one of the primary axes in such structures.

⟨011⟩ Pole Figure (Center Circle) this figure shows a fourfold symmetry with high-intensity spots around the perimeter spaced at 90-degree intervals and one spot in the center. The pattern indicates the grains are oriented in ⟨011⟩ direction which again indicates cubic symmetry.

⟨111⟩ Pole Figure (Right Circle) this figure indicates fourfold symmetry with high-intensity spots at the corners of the square inscribed within the circle. This pattern is typical for a cubic crystal system, were the ⟨111⟩ is a major diagonal of the cube.

Pole Figure indicate the crystallographic directions, indicating the orientation distribution of grains in a polycrystalline material with a cubic crystal structure. The pattern suggests a strong texture, which can affect the material's anisotropic properties and is typically induced by certain processing techniques.

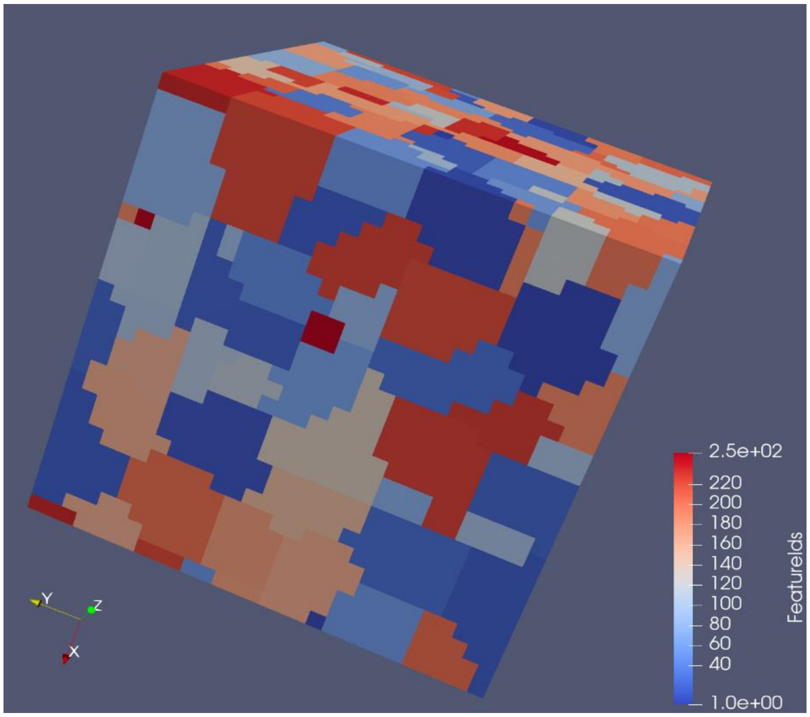

Figure 3.15. 3D plot of Ti-64 with 10μm Grain Size

Figure 3.15 represent, the color map ranges from blue to red, with numerical values alongside the scale bar indicate the values which range from 1.0 (blue) to 2.5 e+02 (red). Red zone represents the dominance of α phase as it is more susceptible to fatigue values will generate higher feature ids in microstructure and blue β phase will generate lower values of feature ids and is represented blue in color.

Due to bigger grain sizes, there is the dark red region in the middle of the microstructure followed by light red regions which increase diagonally throughout the microstructure. It can be predicted that microstructure with 10μm grain size will experience higher stresses and the fatigue crack will propagate quickly within the microstructure.

It can be predicted that Ti-64 microstructure with average grain size of 10μm will exhibit very high homogeneity and fatigue growth in the microstructure will be much higher and will propagate diagonally. It is important to optimize phase distribution in this grain size.

3.12.2 Average Grain Size of 1μm

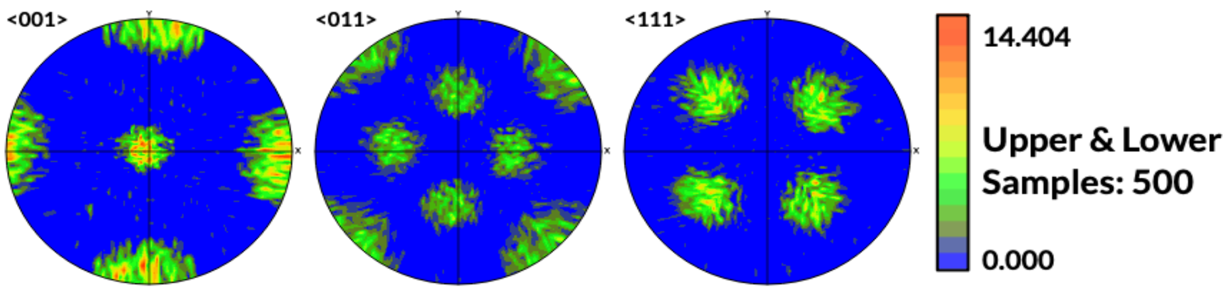

Figure 3.16. Polar Figure of Ti-64 with 1μm Grain Size

Figure 3.16 shows Polar Figure of Ti-64 with 10μm grain size. This figure represents the projections which are used to represent the crystallographic orientation distribution of grains in polycrystalline materials. Three circles represent a different crystallographic direction which are: ⟨001⟩, ⟨011⟩, and ⟨111⟩.

⟨001⟩ Pole Figure (Left Circle) this pole figure shows four high-intensity spots at the poles of the circle and one high intensity spot at the center. This indicates that many grains are oriented such that their axis aligns with these directions. The symmetry suggests a cubic crystal structure as ⟨001⟩ is one of the primary axes in such structures.

⟨011⟩ Pole Figure (Center Circle) this figure shows a fourfold symmetry with high-intensity spots around the perimeter spaced at 90-degree intervals and one spot in the center. The pattern indicates the grains are oriented in ⟨011⟩ direction which again indicates cubic symmetry.

⟨111⟩ Pole Figure (Right Circle) this figure indicates fourfold symmetry with high-intensity spots at the corners of the square inscribed within the circle. This pattern is typical for a cubic crystal system, were the ⟨111⟩ is a major diagonal of the cube.

Pole Figure indicate the crystallographic directions, indicating the orientation distribution of grains in a polycrystalline material with a cubic crystal structure. The pattern suggests a strong texture, which can affect the material's anisotropic properties and is typically induced by certain processing techniques.

Figure 3.17 represent, the color map ranges from blue to red, with numerical values alongside the scale bar indicate the values which range from 1.0 (blue) to 2.4 e+02 (red). Red zone represents the dominance of α phase as it is more susceptible to fatigue values will generate higher feature ids in microstructure and blue β phase will generate lower values of feature ids and is represented blue in color.

Due to smaller grain size, it is clear from the plot received that there will be slow propagation of the crack within the microstructure. There is significant presence of blue region in the microstructure which helps us to predict that grains will be β dominant and grains will be having higher formability and ductility for accommodating higher strains. Light blue regions in the plot indicate that there is slow growth of fatigue crack within the microstructure. As, grains are small there is more optimized distribution of phases within the microstructure and microstructure will have more fatigue resistance.

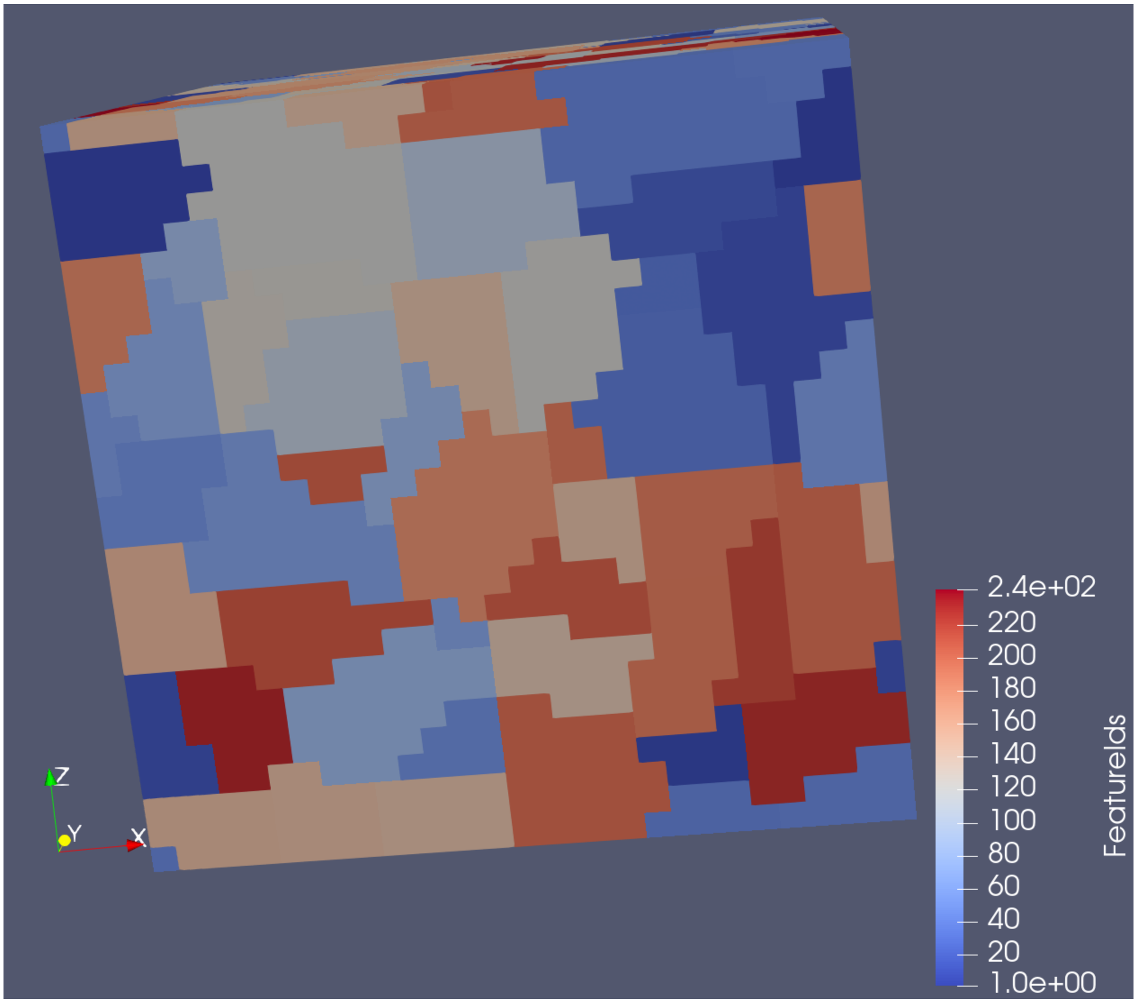

Figure 3.17. 3D plot of Ti-64 with 1μm Grain Size

It can be predicted that Ti-64 microstructure with average grain size of 1μm will exhibit less homogeneity and fatigue growth in the microstructure will be much lower and will propagate slowly. It will withstand a greater number of fatigue cycles as compared to microstructure with 10μm grain size.

3.12.3 Comparative Plots Between 1μm and 10μm

In this section comparison between cubic equiaxed microstructure, random equiaxed microstructure, rolled equiaxed microstructure with grain size of 1 micrometer and 10 micrometer is considered and comparison plot has been plotted.

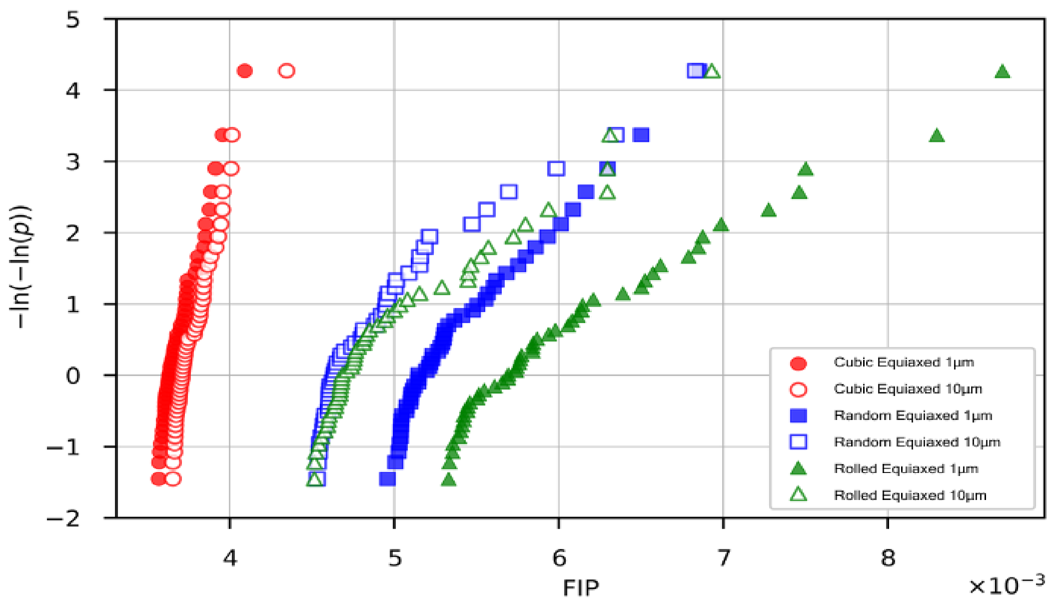

Figure 3.18. Comparative plot of Ti-64 with 1μm and 10μm Grain Size

X-axis of the plot shown in Figure 3.18. represents Fatigue Indicator Parameter (FIP), which is used to predict fatigue damage. The values are in the range of $4x10^{-3}$ to $7x10^{-3}$. Y-axis represents transformed version of probability density function of FIP values, often used in extreme value statistics to assess the distribution of extreme values. Plotting this comparison will help to predict the highest FIP values which are critical for fatigue analysis.

Filled red circles represent cubic microstructure with 1 micrometer grains, open red circles represent cubic microstructure with 10 micrometer grains. Filled blue squares represent random microstructure, with 1 micrometer grains open blue squares represent random microstructure with 10 micrometer grains. Filled green triangles represent rolled microstructure with 1 micrometer grains, open green triangles represent rolled microstructure with 10 micrometer grains.

Data points are clustered into groups based on the type of microstructure (cubic, random, rolled) and grain shape (1 micrometer vs. 10 micrometer). Each group depicts a distinct range of FIP values and probability density transformations.

Cubic microstructures with 1 micrometer grain shape (Filled Circles) have lowest FIP values, indicate that it has better resistance of fatigue damage. Cubic microstructure with 10 micrometer grain shape (Open Circles) are more prone to fatigue damage showing higher FIP values in the plot.

Random microstructures with 1 micrometer grain shape (Filled Squares) have higher FIP values than cubic 1µm and 10 µm indicating that random equiaxed microstructure has moderate fatigue resistance. Random microstructures with 10 µm grain shape (Open Squares) have higher FIP values than 1µm counterparts showing they are more susceptible to fatigue damage.

Based on the plot Rolled microstructure with 1µm grain shape (Filled Triangles) has higher FIP values compared to both random and cubic microstructures. Rolled microstructures with 10µm grain shape (Open Triangles) has highest FIP values among all the other shapes.

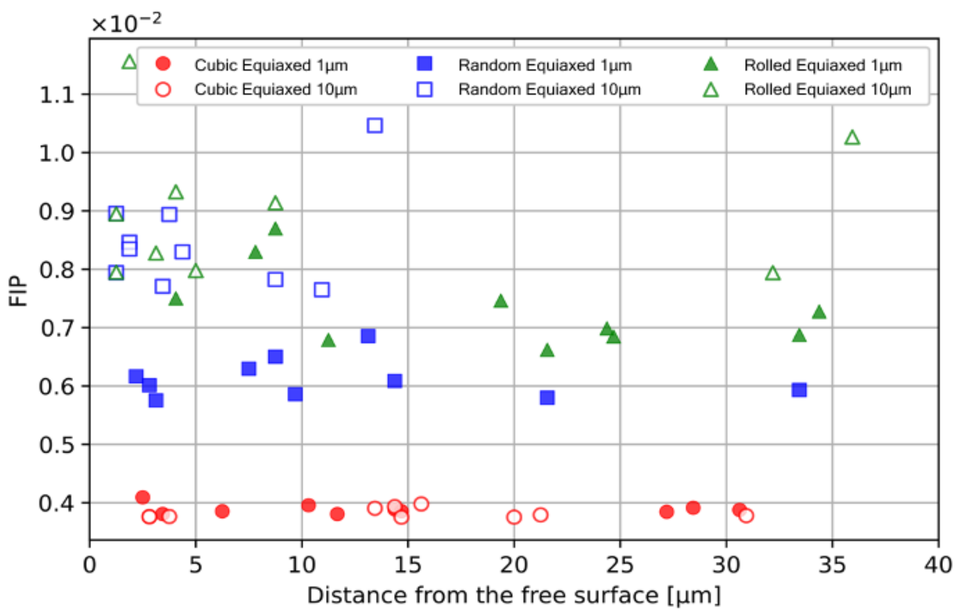

Figure 3.19. Distance of FIPs from Free surface.

The plot in Figure 3.19. shows the change in FIP values as a function of distance from the free surface, which are more critical for predicting fatigue life of microstructure by taking into consideration effect of surface and subsurface interaction under cyclic loading. X-axis represents

(Distance from the free surface [2, 13]) and Y-axis represent FIPs which help to predict the fatigue damage of the microstructure throughout the depth. Values range from 0.4×10^{-2} to 1.0×10^{-2}.

Filled red circles represent cubic microstructure with 1μm grain size, open red circles represent cubic microstructure with 10μm microstructure boundary conditions. Filled blue squares represent random 1μm microstructure, open blue squares represent random 10μm microstructure. Filled green triangles represent rolled 1μm microstructure, open green triangles represent rolled 10μm boundary condition.

Cubic microstructure with 1μm grain size (Filled Circles) shows consistently low values (around 0.4×10^{-2}) indicating good fatigue resistance throughout the depth of microstructure.
Cubic microstructure with 10μm grain size (open circles) shows similar values, suggesting that fatigue damage do not significantly increase for cubic microstructures.

Random microstructure with 1μm grain size (Filled Squares) has higher FIP values ranging from 0.5 to 0.7×10^{-2} indicating that it is more susceptible to fatigue damage compared to cubic microstructures. Random microstructures with 10μm grain size (Open squares) have higher FIP values up to 1.0×10^{-2} indicating that microstructure has increased fatigue damage near the free surface.

Rolled microstructure with 1μm grain size (Filled Triangles) has high values ranging from 0.6 to 0.9×10^{-2} indicating significantly higher susceptibility for fatigue damage. Rolled microstructure with 10μm grain size (Open Triangles) has the greatest susceptibility to fatigue damage.

3.12.4 Experimental Curves

In this section experimental S-N curves of Ti-64 alloy are considered which can directly compared to the model results included in this thesis work. S-N curve illustrates the relationship between maximum stress and the number of cycles to failure under cyclic loading conditions.

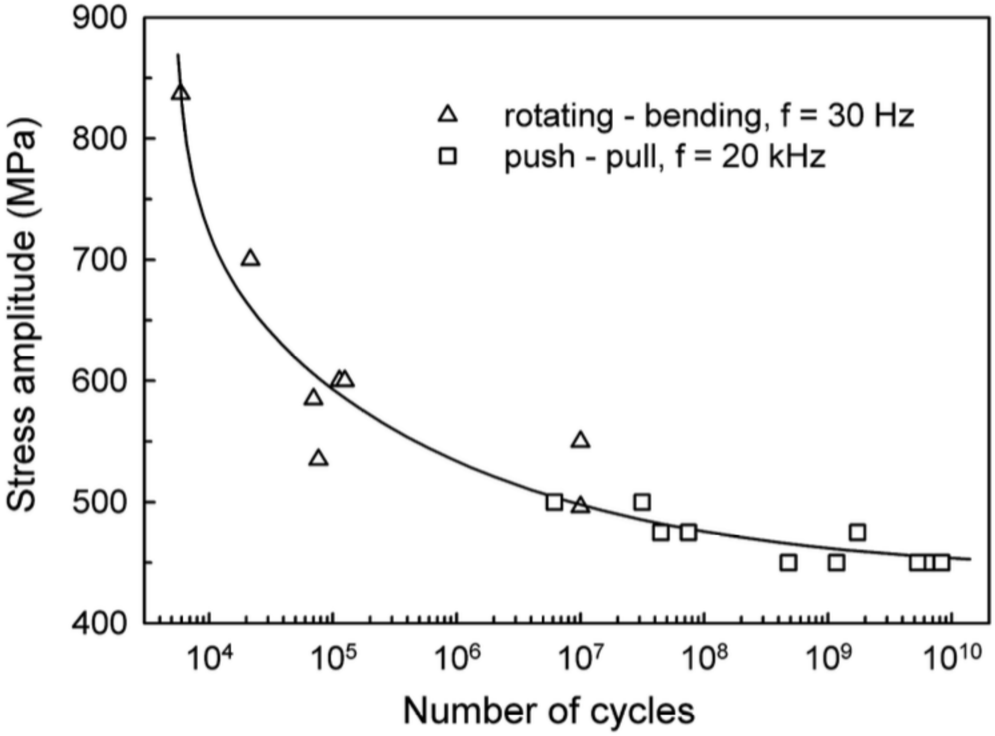

Figure 3.20. S-N plot of Ti-64 [22]

X-axis represents the horizontal axis, plotted on a logarithmic scale, represents the number of cycles the microstructure can endure before failure. Y-axis represents the stress amplitude applied to the material during cyclic loading.

High-Cycle Fatigue (HCF) occurs at 10^6 to 10^{10} the curve flattens out indicating that the microstructure has reached the endurance limit. Under this limit microstructure can withstand infinite number of cycles.

Low-Cycle Fatigue (LCF) occurs at 10^3 to 10^5 the stress amplitude is higher. In this region the stress levels are higher stress levels that cause failure after a relatively low number of cycles.

The point where the curve becomes horizontal indicates the endurance limit of the microstructure. Ti-64 is around 450-500 MPa, as seen from the flattening of the curve at higher cycle counts.

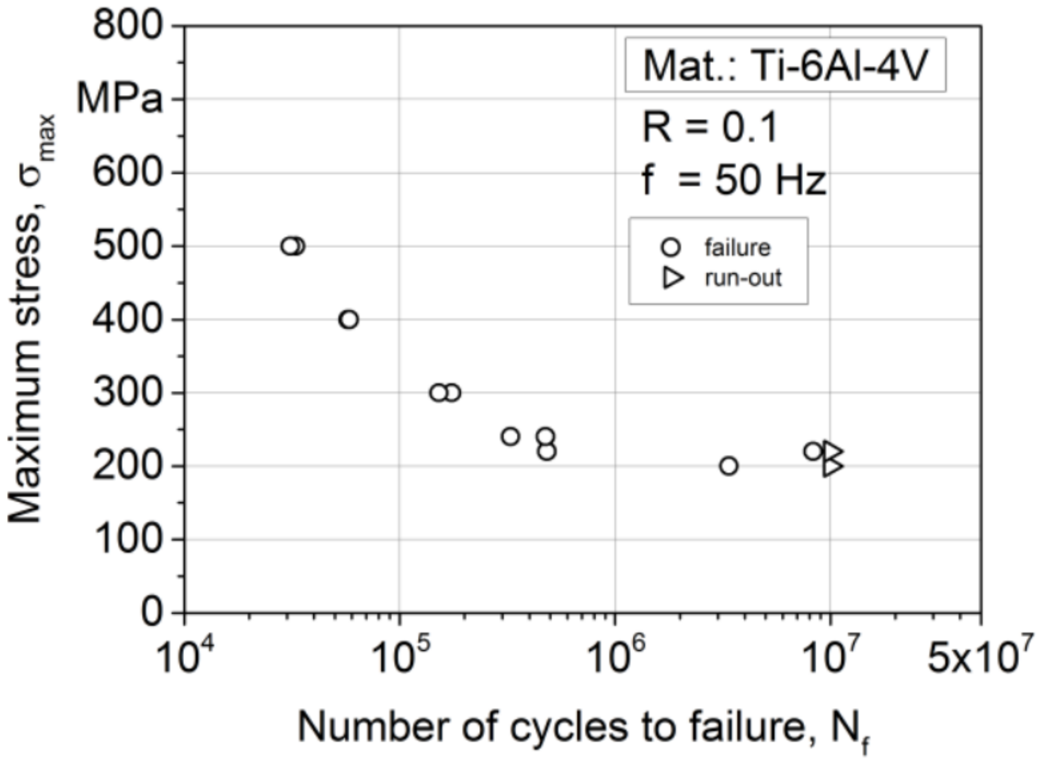

Figure 3.21. S-N plot of As-Printed Ti-64 [23]

X-axis is plotted on a logarithmic scale; represents the number of cycles the material can endure before failure. Y-axis represents the maximum stress applied to the material during cyclic loading.

Stress ration R is given as 0.1. This ratio is defined as the minimum stress divided by the maximum stress in a loading cycle. R value of 0.1 means that minimum stress is 10% of the maximum stress.

Frequency of cyclic loading is specified as 50 Hz, meaning the microstructure in the experimental Ti-64. Meaning the material is subjected to 50 load cycles per second.

The circles indicate the stress levels and corresponding number of cycles at which the material failed. These points help to define the descending part of the S-N curve.

Triangles indicate the stress levels where the material did not fail after many cycles. These points suggest the material's endurance limit.

S-N curve is essential for predicting the fatigue life of components made from Ti-64. These curves help to determine safe stress levels in the microstructure which is being designed. It helps to build optimized microstructure which will not fail under cyclic loading.

For Ti-64 endurance limit is around 250-300 MPa. This experiment which is carried out in [23] closely aligns with the as-printed model created in sections 3.1.1 and 3.1.2. Because of the less optimized phase distribution martensitic α' phase prevails and makes the microstructure tough which causes microstructure to fail in fatigue at lower stress levels.

The PRISMS-Fatigue framework is designed to provide detailed, microstructure-based insights into fatigue behavior, focusing on the underlying mechanisms at the grain and phase levels. While S-N curves offer a macroscopic view of fatigue life under constant amplitude loading, PRISMS-Fatigue aims to capture the complexity of real-world fatigue processes, including variable amplitude and multi-axial loading, and the influence of microstructural features. These detailed simulations and predictions go beyond what is typically represented in traditional S-N curves, making the direct plotting of S-N curves less relevant within this advanced computational framework.[4]

3.13 Discussions

Comparison is done between periodic and free surface boundary conditions. Which gives probability of volume averaged FIPs which occur for each microstructure type.

Based on the results achieved, FIPs are stable and generate constant slope in Cubic microstructure in periodic and free surface boundary conditions. It can be observed that the FIPs which lie in the lower probability region try to fit in the straight line. Whereas FIPs in the higher probability region having varying slopes which is been validated by work done by Tang Gu and Krzysztof [5].

Based on the data received from the simulations in 3.8 Graphical Representation of FIPs in sub-banded microstructure it can be predicted that threshold for maximum FIPs in Cubic periodic microstructure and for Cubic Free surface microstructure is 0.0025. It can be predicted that the

68.8% probability region of FIPs will fall into region between -1.54 to 1.2 and 95.5% probability will lie in the region 1.21 to 3.00. This results coincide with Gumbel and EVD distribution [5].

Random periodic microstructure the initiation of FIP starts at the max strain cycles when, Max FIP is spotted at 0.005. Low probability region lies for -1.54 to 0.91 as the linear slope is analyzed based on results which is 68.8% which follows Gumbel fit till region near 0.91 there is massive change in the slope inclination. 95.5% probability lies in between 0.91 to 2.1 at 0.006 FIP value.

Random free microstructure the initiation of FIP starts at the max strain cycles when, Max FIP is spotted at 0.0058. Low probability region lies for -1.54 to 0.5 which is 68.8% and follows Gumbel by following linear increase in the slope inclination. 95.5% probability lies in between 0.5 to 2 at 0.008 FIP value.

Rolled Periodic microstructure the initiation of FIP starts at the max strain cycles when, Max FIP is spotted at 0.0052. Low probability region lies from -1.54 to -0.92 which is 68.8% which follows Gumbel fit and shows the linear slope. 95.5% probability lies in between -0.92 to 1.5 at 0.0065 FIP value.

Rolled Free microstructure the initiation of FIP starts at the max strain cycles when, Max FIP is spotted at 0.006. Low probability region lies from -1.54 to -0.8 which is 68.8% which follows Gumbel fit and shows the linear slope. 95.5% probability lies in between -0.8 to 1 at 0.008 FIP value.

30SVEs for each type of microstructure have plotted and then the graph is plotted using EVD and Gumbel method. Based on simulation results highest value FIPs have been plotted. Results show that they follow the patterns Cubic periodic Ti-64 microstructure is most stable as grains are closely bonded.

Value of FIPs mainly vary due to grain sizing and grain orientation for max shear strain. As seen in the results it can be predicted that since the Rolled Free surface periodic microstructure has longer grain size as well as larger boundaries it has high probability of FIPs occurring in the microstructure. It is been validated by the results achieved by this work which coincides with work done in [5] as well [24].

Distance from free surface plot as shown in 3.10 Distance of FIPs from Free surfaceproves the most for all the types of grain structure lie in between 0.5 to 25 micrometers which can be validate by comparing with previous work done. Straining plays an important role in determining the distance from the free surface. At distance of 20 micrometers there is negligible free surface effect on the microstructure. FIPs at lower strain levels exceed 20 micrometers threshold and values at higher strain level are spotted at the distance which is less than 20 micrometers coincides with work done in[24].

In gamma plane simulation in anisotropic crystal structure of FIPs play an important role in plotting the shape of the contours. Previous work done my Stopka and McDowell [24] they demonstrate the complex material behavior and demonstrate the presence of free surface under uniaxial straining hence it validates plot which has been plotted which results into distinct contour plots in 3.11 Gamma Plane Simulation

Based on the study done during this thesis and previous work done it can be predicted that for Ti-64 Fatigue experiments fatigue life are longer in shear strain rather than uniaxial straining or loading. It has been observed that uniaxial straining in Ti-64 exceeds equiaxial straining which results improvement in stress ratio of pure titanium and Ti-64 in the microstructure. Which show positive effect on the fatigue life of the microstructure.

Comparison between Ti-64 microstructures with grain size of 1μm and grain size of 10μm it can be predicted that cubic equiaxed microstructure with grain size 1μm will show highest fatigue resistance as compared to microstructure with 10μm grain size. It is because smaller grains with same size and orientation generally act as barriers to dislocation motion in comparison with larger grain size. Hence, based on the results received it can be predicted that Ti-64 microstructures with grain size 1μm are better in fatigue resistance as compared to Ti-64 microstructures with grain size of 10μm.

4. CONCLUSIONS

- Cubic Periodic & Free Surface microstructure will have higher fatigue resistance, as they have more optimized grain structure compared to Random Periodic & Free Surface microstructure as well as Rolled Periodic & Free Surface microstructure.

- Cubic Equiaxed & Elongated microstructure will have higher fatigue resistance, as they have more optimized grain structure which will exhibit higher ductility under shear strain compared to Random Equiaxed & Elongated microstructure as well as Rolled Equiaxed & Elongated microstructure.

- Ti-64 microstructures with grain size of 1μm and grain size of 10μm it can be predicted that cubic equiaxed microstructure with grain size 1μm will show highest fatigue resistance as compared to microstructure with 10μm grain size. It is because smaller grains with same size and orientation generally act as barriers to dislocation motion in comparison with larger grain size. Hence, based on the results received it can be predicted that Ti-64 microstructures with grain size 1μm are better in fatigue resistance as compared to Ti-64 microstructures with grain size of 10μm

5. CONTRIBUTIONS

- To conduct the fatigue analysis on Ti-64 alloy various grain boundary orientations were studied and implemented in Dream-3D software to create the microstructure with different orientations. In this work Ti-64 microstructure was created in three different orientations: Cubic Equiaxed, Random Equiaxed and Rolled Equiaxed.

- Microstructure which is created in Dream-3D is exported to Prisms Plasticity Framework where the microstructure is modeled under the specific loading conditions. Ti-64 microstructure was simulated by considering features like grain size, phase distribution and texture. Simulated data for plastic deformation for all the three-microstructure orientation is stored and studied

- Prisms Fatigue framework uses this data to predict fatigue life of the microstructure considering the high-cycle fatigue (HCF) and low-cycle fatigue (LCF) based on which the damage over repeated loading cycled is predicted considering the microstructure texture

- In this study the data of all the three-grain orientation is plotted together in order give the comparative analysis of all the three-microstructure orientation

- Fatigue Indicator Parameters are used to identify the regions where fatigue damage will start and how the fatigue crack will propagate for each slip plane. Based on the results received the force at which crack can be predicted also number of cycles required to meet the failure can also be predicted

- This model also predicts the distance at which the fatigue crack will initiate from the free surface so that it is easy to predict the region which is weaker and can help to prevent the failure of microstructure by predicting transition from stage-1 cracking to stage-2 cracking

6. LIMITATIONS

Frame-work limitations: Although current model has can predict fatigue life of Ti-64 it has few limitations:

- Results do not hold true if the grain boundary conditions change or there is change in orientation of slip planes

- Simulations which need high number of fatigue cycle need greater computational power which might cause results to vary, and accuracy of results received needs to be verified

- Frame-work is built in such a way that it only reads data which is been provided by the user, real time complexities might be captured unless microstructure is remodeled

- Materials which have severe anisotropy or heterogeneity can be difficult to model accurately due to complex interaction between different properties and phases

REFERENCES

[1] W. Schütz, "A history of fatigue," *Engineering Fracture Mechanics,* vol. 54, no. 2, pp. 263-300, 1996/05/01/ 1996, doi: https://doi.org/10.1016/0013-7944(95)00178-6.

[2] P. J. E. Forsyth, "Exudation of Material from Slip Bands at the Surface of Fatigued Crystals of an Aluminium–Copper Alloy," *Nature,* vol. 171, no. 4343, pp. 172-173, 1953/01/01 1953, doi: 10.1038/171172a0.

[3] A. Fatemi and D. F. Socie, "A CRITICAL PLANE APPROACH TO MULTIAXIAL FATIGUE DAMAGE INCLUDING OUT-OF-PHASE LOADING," *Fatigue & Fracture of Engineering Materials & Structures,* vol. 11, no. 3, pp. 149-165, 1988, doi: https://doi.org/10.1111/j.1460-2695.1988.tb01169.x.

[4] M. Yaghoobi, K. S. Stopka, A. Lakshmanan, V. Sundararaghavan, J. E. Allison, and D. L. McDowell, "PRISMS-Fatigue computational framework for fatigue analysis in polycrystalline metals and alloys," *npj Computational Materials,* vol. 7, no. 1, p. 38, 2021/03/17 2021, doi: 10.1038/s41524-021-00506-8.

[5] T. Gu, K. S. Stopka, C. Xu, and D. L. McDowell, "Prediction of maximum fatigue indicator parameters for duplex Ti–6Al–4V using extreme value theory," *Acta Materialia,* vol. 188, pp. 504-516, 2020/04/15/ 2020, doi: https://doi.org/10.1016/j.actamat.2020.02.009.

[6] M. A. Galindo-Fernández, K. Mumtaz, P. E. J. Rivera-Díaz-del-Castillo, E. I. Galindo-Nava, and H. Ghadbeigi, "A microstructure sensitive model for deformation of Ti-6Al-4V describing Cast-and-Wrought and Additive Manufacturing morphologies," *Materials & Design,* vol. 160, pp. 350-362, 2018/12/15/ 2018, doi: https://doi.org/10.1016/j.matdes.2018.09.028.

[7] M. Zhang *et al.*, "On the damage tolerance of 3-D printed Mg-Ti interpenetrating-phase composites with bioinspired architectures," *Nature Communications,* vol. 13, no. 1, p. 3247, 2022/06/06 2022, doi: 10.1038/s41467-022-30873-9.

[8] N. C. Bellinger and M. Liao, "8 - Corrosion and fatigue modeling of aircraft structures," in *Corrosion Control in the Aerospace Industry*, S. Benavides Ed.: Woodhead Publishing, 2009, pp. 172-191.

[9] S. Forth, J. Newman, and R. Forman, "Evaluation of fatigue crack thresholds using various experimental methods," *ASTM Special Technical Publication,* vol. 1461, p. 203, 2005.

[10] Y. Murakami, T. Takagi, K. Wada, and H. Matsunaga, "Essential structure of S-N curve: Prediction of fatigue life and fatigue limit of defective materials and nature of scatter," *International Journal of Fatigue,* vol. 146, p. 106138, 2021/05/01/ 2021, doi: https://doi.org/10.1016/j.ijfatigue.2020.106138.

[11] C. Amzallag, J. P. Gerey, J. L. Robert, and J. Bahuaud, "Standardization of the rainflow counting method for fatigue analysis," *International Journal of Fatigue*, vol. 16, no. 4, pp. 287-293, 1994/06/01/ 1994, doi: https://doi.org/10.1016/0142-1123(94)90343-3.

[12] H. Al-Karawi, R. U. F. von Bock und Polach, and M. Al-Emrani, "Fatigue life extension of existing welded structures via high frequency mechanical impact (HFMI) treatment," *Engineering Structures*, vol. 239, p. 112234, 2021/07/15/ 2021, doi: https://doi.org/10.1016/j.engstruct.2021.112234.

[13] P. Kumar, O. Prakash, and U. Ramamurty, "Micro-and meso-structures and their influence on mechanical properties of selectively laser melted Ti-6Al-4V," *Acta Materialia*, vol. 154, pp. 246-260, 2018/08/01/ 2018, doi: https://doi.org/10.1016/j.actamat.2018.05.044.

[14] J. A. Tamayo, M. Riascos, C. A. Vargas, and L. M. Baena, "Additive manufacturing of Ti6Al4V alloy via electron beam melting for the development of implants for the biomedical industry," *Heliyon*, vol. 7, no. 5, p. e06892, 2021/05/01/ 2021, doi: https://doi.org/10.1016/j.heliyon.2021.e06892.

[15] R. Cottam *et al.*, "Diffraction Line Profile Analysis of 3D Wedge Samples of Ti-6Al-4V Fabricated Using Four Different Additive Manufacturing Processes," *Metals*, vol. 9, p. 60, 01/09 2019, doi: 10.3390/met9010060.

[16] M. A. Groeber and M. A. Jackson, "DREAM.3D: A Digital Representation Environment for the Analysis of Microstructure in 3D," *Integrating Materials and Manufacturing Innovation*, vol. 3, no. 1, pp. 56-72, 2014/12/01 2014, doi: 10.1186/2193-9772-3-5.

[17] C. P. Przybyla and D. L. McDowell, "Microstructure-sensitive extreme-value probabilities of high-cycle fatigue for surface vs. subsurface crack formation in duplex Ti–6Al–4V," *Acta Materialia*, vol. 60, no. 1, pp. 293-305, 2012/01/01/ 2012, doi: https://doi.org/10.1016/j.actamat.2011.09.031.

[18] P. Bocchetta, L. Chen, J. Tardelli, A. Reis, F. Almeraya Calderon, and P. Leo, "Passive Layers and Corrosion Resistance of Biomedical Ti-6Al-4V and β-Ti Alloys," *Coatings*, vol. 11, 04/16 2021, doi: 10.3390/coatings11050487.

[19] G.-z. Quan *et al.*, "A Characterization for the Constitutive Relationships of 42CrMo High Strength Steel by Artificial Neural Network and its Application In Isothermal Deformation," *Materials Research*, vol. 17, pp. 0-0, 09/01 2014, doi: 10.1590/1516-1439.211713.

[20] M. W. Brown and K. J. Miller, "A Theory for Fatigue Failure under Multiaxial Stress-Strain Conditions," *Proceedings of the Institution of Mechanical Engineers*, vol. 187, no. 1, pp. 745-755, 1973, doi: 10.1243/pime_proc_1973_187_161_02.

[21] M. M. Raza, A. R. Dezfoli, and Y.-L. Lo, "3D Multi-Track and Multi-Layer Epitaxy Grain Growth Simulations of Selective Laser Melting," *Materials,* 11/30 2021, doi: 10.3390/ma14237346.

[22] M. Janeček *et al.*, "The Very High Cycle Fatigue Behaviour of Ti-6Al-4V Alloy," *Acta Physica Polonica A*, vol. 128, pp. 497-503, 10/01 2015, doi: 10.12693/APhysPolA.128.497.

[23] E. Wycisk, C. Emmelmann, S. Siddique, and F. Walther, "High Cycle Fatigue (HCF) Performance of Ti-6Al-4V Alloy Processed by Selective Laser Melting," *Advanced Materials Research*, vol. 816-817, pp. 134-139, 09/23 2013, doi: 10.4028/www.scientific.net/AMR.816-817.134.

[24] K. S. Stopka and D. L. McDowell, "Microstructure-sensitive computational multiaxial fatigue of Al 7075-T6 and duplex Ti-6Al-4V," *International Journal of Fatigue*, vol. 133, p. 105460, 2020/04/01/ 2020, doi: https://doi.org/10.1016/j.ijfatigue.2019.105460.

APPENDIX

Prisms Fatigue Scripts

Generate Microstructure

First python script needed to start the simulation of the microstructure is Generate Microstructure. This script reads in the Dream-3D file and generates pickle files which are used to calculate FIPs**.** Generate Microstructure is called it executes main function; and then the code is executed.

```
def main():
    # Run from command prompt


    ''' Specify directories and paths '''
    # Directory where microstructure data should be generated and pre-processed
    # This command creates a directory in the same location as the "PRISMS-Fatigue" directory with python scripts and DREAM.3D files
    directory = os.path.dirname(DIR_LOC) + '/tutorial/test_7'

    # Alternatively, the directory can be expressed as an absolute path as:
    # directory = r'C:\Users\stopk\Documents\GitHub\PRISMS-Fatigue\tutorial\test_run_1'

    # Location of DREAM.3D input file; should consist of only the "StatsGenerator" and "Write DREAM.3D Data File"
    # "StatsGenerator" inputs include grain size distribution, crystallographic texture, grain morphology, etc.
    # Six ".dream3d" files are included in PRISMS-Fatigue
    d3d_input_file = os.path.abspath(DIR_LOC) + '/Al7075_random_texture_equiaxed_grains.dream3d'

    # Once again, this may be specified using an absolute path as:
    # d3d_input_file = r'C:\Users\stopk\Documents\GitHub\PRISMS-Fatigue\Al7075_cubic_texture_equiaxed_grains.dream3d'

    # Average grain size as determined in the "StatsGenerator" filter of the .dream3d file above
    # Used for automated band and sub-band sizing as shown below but which can be overwritten by the user
    # Therefore, this does NOT change the grain size generated and only affects the way in which microstructures are banded and sub-banded!
    avg_grain_size = 0.014 # millimeters

    # Location of DREAM.3D .json pipeline
    # This can be modified by the user to include additional outputs
    d3d_pipeline_path = os.path.abspath(DIR_LOC) + '/Dream3D_microstructure_pipeline.json'

    # Once again, this may be specified using an absolute path as:
1|   # d3d_pipeline_path = r'C:\Users\stopk\Documents\GitHub\PRISMS-Fatigue\Dream3D_microstructure_pipeline.json'

    # Location of DREAM.3D 'PipelineRunner.exe' file; this should be in the DREAM.3D program folder
    d3d_executable_path = '/Users/sanketkulkarni/Desktop/Contents/bin/PipelineRunner'
```

Figure A 1. Generate Microstructure Main Function

Specify Directories and Path

```python
''' Specify directories and paths '''
# Directory where microstructure data should be generated and pre-processed
# This command creates a directory in the same location as the "PRISMS-Fatigue" directory with python scripts and DREAM.3D files
directory = os.path.dirname(DIR_LOC) + '/tutorial/test_7'

# Alternatively, the directory can be expressed as an absolute path as:
# directory = '\Documents\GitHub\PRISMS-Fatigue\tutorial\test_7'

# Location of DREAM.3D input file; should consist of only the "StatsGenerator" and "Write DREAM.3D Data File"
# "StatsGenerator" inputs include grain size distribution, crystallographic texture, grain morphology, etc.
# Six ".dream3d" files are included in PRISMS-Fatigue
d3d_input_file = os.path.abspath(DIR_LOC) + '/Al7075_random_texture_equiaxed_grains.dream3d'

# Once again, this may be specified using an absolute path as:
# d3d_input_file = r'C:\Users\stopk\Documents\GitHub\PRISMS-Fatigue\Al7075_cubic_texture_equiaxed_grains.dream3d'

# Average grain size as determined in the "StatsGenerator" filter of the .dream3d file above
# Used for automated band and sub-band sizing as shown below but which can be overwritten by the user
# Therefore, this does NOT change the grain size generated and only affects the way in which microstructures are banded and sub-banded!
avg_grain_size = 0.014 # millimeters

# Location of DREAM.3D .json pipeline
# This can be modified by the user to include additional outputs
d3d_pipeline_path = os.path.abspath(DIR_LOC) + '/Dream3D_microstructure_pipeline.json'

# Once again, this may be specified using an absolute path as:
 # d3d_pipeline_path = r'C:\Users\stopk\Documents\GitHub\PRISMS-Fatigue\Dream3D_microstructure_pipeline.json'

# Location of DREAM.3D 'PipelineRunner.exe' file; this should be in the DREAM.3D program folder
d3d_executable_path = '/Users/sanketkulkarni/Desktop/Contents/bin/PipelineRunner'
```

Figure A 2. Section one of main function: (Specify Directories and Paths)

Code flow of Section-1: Specify Path and Directory.

- Specifying directory where the results are generated.
- Specifying Dream 3D path to read, Dream 3D file as input.
- Read the average grain size from Dream3D and then band and sub-band the structure by mentioning the desired size.
- Mentioning the Dream-3d pipeline path for the execution of additional outputs
- Mentioning the Pipeline Runner path which helps to run Dream-3d pipeline.

After successful execution of this section of script, prisms fatigue framework can read and store data from Dream-3d file. As well as create the sizing of bands and sub-bands in the microstructure.

Specifying Size and Shape

In this section of main function, script generates instantiations of microstructures with specified size of each instantiation. It also creates the number of elements for each instantiation which helps in calculating slip factor for calculating Fatigue Indicator Parameters (FIPs).

```
''' Specify desired microstructure size and shape '''
# Size of microstructure instantiations in millimeters, in the X, Y, and Z directions, respectively.
size  = np.asarray([.0725,.0725,.0725])

# Shape of microstructure instantiations (number of voxels/elements), in the X, Y, and Z directions, respectively.
# IMPORTANT: at this point, only CUBIC voxel functionality supported even with a non-cubic microstructure
# I.e., size = [.05, .1, .025] and shape = [50, 100, 25] is acceptable
shape = np.asarray([50,50,50])

# Number of microstructure instantiations to generate using DREAM.3D
num_instantiations = 30
```

Figure A 3. Specifying Size and Shape

Specifying details of banding and sub-banding

Code flow of Section: Specify details of banding and sub-banding.

- Specifying number of elements in each sub-band
- Formulating number for voxel sub-banding
- Modelling the band thickness of each sub-band
- Creating crystallographic slip planes for FIP volume avg

Last step in this section is, computing Kosher grain centroid, it usually helps in setting up the periodicity of the microstructure which also reduces computing type.

```
''' Specify details of banding and sub-banding process '''
# Specify the number of elements in each sub-band for volume averaging
# Please see the references below for more information
# WARNING!: If this is too low for very refined grains, this module will take a long time to run!
# This is because it attempts to determine all UNIQUE combinations of some number of neighboring elements

# NOTE: Aim for ~8-10% of the average grain volume as the num_vox, as specified below
# This is especially important when comparing microstructures with different grain sizes!
num_vox_percentage = 0.10

# This line calculates num_vox to be "num_vox_percentage" percent of the predicted average number of elements per grain
num_vox = np.around(np.prod(shape) / (np.prod(size) / ( (1.0/6.0) * np.pi * avg_grain_size ** 3  ) ) * num_vox_percentage).astype(int)

# Comment out the above line and uncomment the line below to manually set the number of elements per sub-band
# num_vox = 8

# Specify the thickness of bands in terms of number of elements
# Ideally, this should result in approximately 6 bands for coarser grains (~100 elements per grain)
# NOTE: This should also be ~one or a few micrometers in thickness based on experimental observations of slip bands
# See reference below, Castelluccio and McDowell

# This line calculates the band thickness IN MULTIPLES OF element thickness
band_thickness = np.around( avg_grain_size / ( 6 * size[0]/shape[0]) )
if band_thickness < 1:
    # The microstructure is relatively coarse so need to override band thickness to 1 element in width
    print('Setting band thickness to 1 element in width')
    band_thickness = 1.0

# Comment out the above line and uncomment the line below to manually set the band element thickness
# Set as float for subsequent calculations
# band_thickness = 3.0

# Number of crystallographic slip planes for FIP Volume averaging
# There are four slip planes in the Al 7075-T6 material system (see references below)
num_planes = 4

# Specify whether bands in grains should be further assigned to unique sub-bands
# WARNING!: this is slow for a) microstructures with many grains, and 2) very fine grains, i.e., thousands of elements per grain
# NOTE: Microstructure(s) can be created with this intially set to False, and the "gen_microstructures" can be executed with the variable "generate_new_microstructure_files" set to False, so that th
create_sub_bands = True

# Specify whether the centroids of grains split by the microstructure boundary should be manipulated to reflect periodicity
# Setting this to False will substantially increase the speed at which microstructures are pre-processed, but will reduce the accuracy of computed and volume-averaged fatigue indicator parameters do
# Users can set this to False but rerun this script with "generate_new_microstructure_files" set to False and "compute_kosher_grain_centroids" set to True to compute the realistic grain centroids at
compute_kosher_grain_centroids = True
```

Figure A 4. Specifying Details of banding and sub-banding

Specifying Boundary Conditions

```
''' Specify boundary conditions '''
# Boundary conditions, either "periodic" or "free surface", for X,Y,Z directions
# Three possible combinations: 1) all 'periodic', 2) all 'free', or 3) two 'periodic' + one 'free'
face_bc = ['free', 'free', 'free']

# Specify whether DREAM.3D was previously executed on these files
# If set to False, the script will NOT generate new DREAM.3D microstructure(s) and instead process the existing microstructures by reading the .csv and GrainID_#.txt files
# Reasons to set this to False:
#     1) Process the same set of microstructures with a different number of elements per sub-band, and store these in a separate folder. In this case, copy over the .csv and GrainID_#.txt files to a
#     2) Generate a set of ['periodic', 'periodic', 'periodic'] microstructures, and then reprocesses them with one set of faces set to non-periodic, i.e., ['periodic', 'free', 'periodic'], to study
# NOTE: If the variable is set to False, all that is needed in the folder is the DREAM.3D exported .csv and "grainID.txt" files for each microstructure
generate_new_microstructure_files = True

# Print the parameters of this microstructure set to a text file
print_params(directory, size, shape, face_bc, num_vox, band_thickness, num_planes, num_instantiations, d3d_input_file)

# Call to the main function
gen_microstructures(directory, size, shape, face_bc, num_vox, band_thickness, num_planes, create_sub_bands, num_instantiations, generate_new_microstructure_files, compute_kosher_grain_centroids, d3d
```

Figure A 5. Specifying Boundary Condition

In this last section all the boundary conditions are built for each file microstructure file. It also includes the files data which needs to be stored for each instantiation. Hence, script run for the instantiation which are mentioned by the user.

Calculate FIPs

While executing this script main function runs, to calculate FIPs for given parameters and this script is being executed generating 'FS_FIP' files.

```python
def main():

    # Directory where PRISMS-Plasticity results .csv files are stored
    # In the case of gamma plane simulations, this should contain all the folders numbered 0 thru (number_of_folder - 1), each of which contains some number of instantiations simulated at some combinati
    directory = os.path.dirname(DIR_LOC) + '/tutorial/Prisms-Fatigue-Training /MultiaxialFatigue_Al7075T6'

    #directory ='/Users/sanketkulkarni/Documents/GitHub/Fatigue/tutorial/Prisms-Fatigue-Training /Texture_Effect_Al7075T6/random_equiaxed_periodic'

    # Shape of microstructure instantiations (at this point, only CUBIC voxel functionality supported)
    # THIS MUST MATCH THE SHAPE FROM THE 'generate_microstructure.py' SCRIPT!
    shape = np.asarray([30,30,30])

    # Number of microstructure instantiations for which to calculate FIPs
    # THIS MUST MATCH THE SHAPE FROM THE 'generate_microstructure.py' SCRIPT! Otherwise, FIPs will not be computed for all instantiations!
    num_instantiations = 10

    # Specify the FIP to be calculated; default is "FS_FIP"
    # The other FIP that can be calculated uses the plastic shear strain range on each slip system; FIP_type = 'plastic_shear_strain_range'
    FIP_type = 'FS_FIP'

    # Define the two Fatemi-Socie (FS) FIP parameters; Please see the references below for more information
    k_fip   = 10.0
    sigma_y = 517.0

    FIP_params = [k_fip, sigma_y]

    # For an fcc material, there are 12 slip systems for each element and therefore 12 FIPs per element
    num_slip_systems = 12

    # Specify whether this folder contain multiple instantiations to generate the multiaxial Gamma plane
    # This requires additional post-processing of PRISMS-Plasticity output files to calculate macroscopic plastic strain tensors
    gamma_plane_simulations = True

    # Specify whether to append the .vtk file generated by DREAM.3D to visualize the highest FIP per element
    vtk_visualize_FIPs = False

    # Number of multiaxial strain state and magnitude folders, i.e., strain states simulated
    # This is only required if calculating the necessary files to generate a multiaxial gamma plane
    num_gamma_plane_folders = 95

    # Specify whether PRISMS-Plasticity performs simulations with fully integrated elements
    # This corresponds to the "Order of quadrature" parameter in the PRISMS-Plasticity .prm file
    full_integration = False

    if gamma_plane_simulations:

        # Iterate through folders containing result files from multiaxial simulations
        for jj in range(num_gamma_plane_folders):
            dirr = os.path.join(directory, str(jj))
            print(dirr)

            for ii in range(num_instantiations):
                # print('Instantiation number %d' % ii)
                import_PRISMS_data(dirr, shape, ii, FIP_type, num_slip_systems, FIP_params, gamma_plane_simulations, full_integration)

    else:
        # Otherwise, compute FIPs for a single folder
        for ii in range(num_instantiations):
            import_PRISMS_data(directory, shape, ii, FIP_type, num_slip_systems, FIP_params, gamma_plane_simulations, full_integration)

    if vtk_visualize_FIPs and not gamma_plane_simulations:
        for ii in range(num_instantiations):
            # Write FIPs to .vtk file for visualization
            append_FIPs_to_vtk(directory, shape, ii, FIP_type, num_slip_systems)
```

Figure A 6. Calculate FIPs main function.

Code Flow of Calculate FIPs

- Directing the script to the folder where prisms plasticity folder has .csv stored.
- Creating shape of the array for each instantiation
- Creating the calculated FIPs and storing it by the name FS_FIPs
- Giving parameters for calculating FIPs

- Selecting the files which needs to be generated which helps in modelling time.

Volume Average FIPs

```
def main():

    # Directory where microstructure FIP .p files are stored:
    directory = os.path.dirname(DIR_LOC) + '/tutorial/Prisms-Fatigue-Training /MultiaxialFatigue_Al7075T6'

    # directory = r'C:\Users\stopk\Documents\GitHub\PRISMS-Fatigue\tutorial\test_run_1'

    # Number of microstructure instantiations in each folder for which to volume average FIPs
    num_instantiations = 10

    # Specify the FIP to be volume averaged
    FIP_type = 'FS_FIP'

    # Specify type of FIP averaging: 'sub_band', 'band', or 'grain'
    averaging_type = 'sub_band'

    # Specify whether this folder contain multiple instantiations to generate the multiaxial Gamma plane
    gamma_plane_simulations = True

    # Number of multiaxial strain state and magnitude folders, i.e., strain states simulated
    # This is only required if calculating necessary files to generate multiaxial gamma plane
    num_gamma_plane_folders = 95

    if gamma_plane_simulations:
        # Iterate through folders containing result files from multiaxial simulations
        for jj in range(num_gamma_plane_folders):
            dirr = os.path.join(directory, str(jj))
            print(dirr)

            for ii in range(num_instantiations):
                call_averaging(ii, dirr, FIP_type, averaging_type, gamma_plane_simulations)

    else:
        # Call function to perform averaging for each instantiation in folder
        for ii in range(num_instantiations):
            call_averaging(ii, directory, FIP_type, averaging_type, gamma_plane_simulations)

if __name__ == "__main__":
    main()
```

Figure A 7. Volume Averaged(main) function.

Code Flow of Volume Average script

- Specifying folders where the pickle files are located.

- Specifying number of instantiations in each folder for which FIPs must be volume averaged.

- Specifying Calculated FIPs file; as well as specifying volume average type for which we want to model microstructure.

‘If’ loop is created towards the end of the function based on if gamma plane is True or False to execute this function. Volume averaged files are formed, and scripts run for instantiations mentioned.

Compile and plot

Directory Locations

```
# Get name of directory that contains the PRISMS-Fatigue scripts
DIR_LOC = os.path.dirname(os.path.abspath(__file__))

locats_Al7075_compare_BC_prisms =   [os.path.dirname(DIR_LOC) + '/tutorial/Texture_Effect_Al7075T6/cubic_equiaxed_periodic',
                                     os.path.dirname(DIR_LOC) + '/tutorial/Prisms-Fatigue-Training /FreeSurface_Effect_Al7075T6/cubic_equiaxed_free_surface',
                                     os.path.dirname(DIR_LOC) + '/tutorial/Texture_Effect_Al7075T6/random_equiaxed_periodic',
                                     os.path.dirname(DIR_LOC) + '/tutorial/Prisms-Fatigue-Training /FreeSurface_Effect_Al7075T6/random_equiaxed_free_surface',
                                     os.path.dirname(DIR_LOC) + '/tutorial/Texture_Effect_Al7075T6/rolled_equiaxed_periodic',
                                     os.path.dirname(DIR_LOC) + '/tutorial/Prisms-Fatigue-Training /FreeSurface_Effect_Al7075T6/rolled_equiaxed_free_surface']


locats_Al7075_compare_shape_prisms = [os.path.dirname(DIR_LOC) + '/tutorial/Texture_Effect_Al7075T6/cubic_equiaxed_periodic',
                                      os.path.dirname(DIR_LOC) + '/tutorial/Prisms-Fatigue-Training /GrainMorphology_Effect_Al7075T6/cubic_elongated_periodic',
                                      os.path.dirname(DIR_LOC) + '/tutorial/Texture_Effect_Al7075T6/random_equiaxed_periodic',
                                      os.path.dirname(DIR_LOC) + '/tutorial/Prisms-Fatigue-Training /GrainMorphology_Effect_Al7075T6/random_elongated_periodic',
                                      os.path.dirname(DIR_LOC) + '/tutorial/Texture_Effect_Al7075T6/rolled_equiaxed_periodic',
                                      os.path.dirname(DIR_LOC) + '/tutorial/Prisms-Fatigue-Training /GrainMorphology_Effect_Al7075T6/rolled_elongated_periodic']
```

Figure A 8. Specifying Directory for comparison of plotting results

In this script it is important to mention, the files which we must compare while plotting the results. Results can be plotted using math ‘compare boundary conditions’ also it can be plotted using by ‘comparing shape functions.’ While plotting results using ‘boundary conditions’: periodic boundaries are compared with free surface boundaries which gives probability comparison of where exactly the extreme value distributed FIPs would be found in the microstructure.

While plotting the comparison with the shape functions equiaxed periodic is plotted in comparison of grain morphology. Which gives us the probability of where the FIPs occur based on the shape.

Main Executing Function of Compile and plot scripts

```python
def main():
    # Specify type of analysis: either 'fip_evd' to plot FIP extreme value distributions (EVDs) or 'surf_dist' to plot the highest FIPs as a function of their distance to the free surface
    analysis_type = 'surf_dist'

    # Specify folder which contains all of the simulation batch folders
    # IMPORTANT: this directory should contain the locations specified at the top of this python script, NOT the individual folders with the instantiations!
    # This script goes through EACH ONE of the folders specified and extracts the relevant information for plotting purposes

    directory = os.path.dirname(DIR_LOC) + '/tutorial'

    # directory = r'C:\Users\stopk\Documents\GitHub\PRISMS-Fatigue\tutorial\test_run_1'

    # Specify which 'material' to plot, i.e., which combination of microstructure folders
    # Please see the top of the "plot_FIPS" function
    mat = 'prisms_compare_bcs'

    # Specify which FIP to import
    FIP_type = 'FS_FIP'

    # Specify which volume averaging scheme to import. By default, the sub-band averaged (SBA) FIPs are used
    # IMPORTANT: this will fail if the FIPs have not yet been averaged in the desired manner (see 'volume_average_FIPs.py' script)
    # Options: 'sub_band', 'band', and 'grain'
    averaging_type = 'sub_band'

    if analysis_type == 'fip_evd':

        # Specify how many of the highest FIPs should be plotted
        n_fip_plot = 50

        # Specify whether FIPs should be fit to the "gumbel" or "frechet" EVD
        plt_type = 'gumbel'

        # Call function to plot FIPs
        plot_FIPS(directory, plt_type, mat, n_fip_plot, FIP_type, averaging_type, save_fig = True)

    elif analysis_type == 'surf_dist':
        # Plot SBA FIP vs distance from free surface:

        # Specify how many of the highest FIPs should be plotted
        n_fip_plot = 10

        # Specify the non-periodic direction (i.e., the set of parallel faces set to traction-free conditions)
        # In the references associated with these scripts (see below), this is set to the 'Y' direction
        non_periodic_dir = 'Y'

        # Specify the size/length of the SVE in the non-periodic direction in mm, to properly locate the FIPs within the microstructure
        SVE_non_periodic_length = 0.0725

        # Call function to plot FIPs
        plot_EVD_FIP_distance(directory, mat, n_fip_plot, FIP_type, averaging_type, non_periodic_dir, SVE_non_periodic_length)

if __name__ == "__main__":
    main()
```

Figure A 9. Main Function of Compile and Plot

- Specifying the analysis for which we need plot i.e., by mentioning ‘fip_evd’ for extreme value distribution. Also, plotting the distance of highest FIPs from the free surface ‘surf_dist’.

- Specifying the folder where all the simulation files are located. Scripts goes through each sub-folders and extracts data which are required for plotting.

- Specifying material that can be used for calculating FIPs.

- Material that can be used are either by comparing boundary conditions or by comparing shape

Multiaxial Gamma plane

- Multiaxial gamma plane computes the fatigue response of a polycrystalline alloys and metals under the various strain states and magnitudes.
- While computing the gamma plane simulation the strain states considered are uniaxial, bi-axial, and pure shear-strain.
- While computing the gamma plane simulation the mesh is refined to simulate the more realistic microstructure.
- Gamma plane script is initiated to generate the ISO-FIP contour plots which are then used to predict the fatigue life behavior of the polycrystal metal or alloy. Which are like work done Brown and Miller to plot ISO-life contours to predict fatigue life.

```
def main():

    # Specify name of directory with simulation folders, each with the same X number of microstructures simulated to some combination of strain state and magnitude, and numbered 0 thru (numb
    directory = os.path.dirname(DIR_LOC) + '/tutorial/Prisms-Fatigue-Training /MultiaxialFatigue_Al7075T6'

    # Specify the number of FIPs to extract from each simulation folder
    num_FIPs_extract = 50

    # Specify how many of the highest FIPs from each batch of simulations should be considered to plot the ISO-FIP contours
    num_read_top_FIPs = 10

    # Specify which FIP to import
    FIP_type = 'FS_FIP'

    # Specify type of FIP averaging: 'sub_band', 'band', or 'grain'
    averaging_type = 'sub_band'

    # Plot the locations of each simulation batch folder in terms of only the response coordinates (x and y position on the gamma plane)
    plot_gamma_plane_locations(directory)

    # This function will extract the 50 highest fips from each folder and store these in a single pickle file.
    # This function is run once to speed up subsequent analysis and plotting
    get_gamma_FIPs(directory, num_FIPs_extract, FIP_type, averaging_type)

    # Plot the gamma plane
    plot_gamma(directory, num_read_top_FIPs, FIP_type, averaging_type)
```

Figure A 10. Main Function of Gamma Plane Simulation

Main Executing function of Gamma plane simulation

Code flow of the script Gamma Plane Simulation script:

- Specify the directory where the multiaxial fatigue folder is stored.
- Specify number of FIPs to extracted from each simulation folder.
- Specify number of highest FIP per grain to generate response at each response co-ordinate.
- Specify FIP type to be imported.
- Specify averaging type so that code can read the file generated from volume averaged function and generate the results.
- Direct the code to the location where the results should be stored.
- Storing the 50 highest FIPs in the single pickle file and then reading the results, this step also helps in increasing the speed of plotting the results.
- After successful execution of all the functions the gamma plane is plotted.